Atmospheric
Chemistry
and Physics
Discussions

1   **Principal component analysis of summertime ground site measurements in the Athabasca oil sands:**

2   **Sources of IVOCs**

3

4   Travis W. Tokarek[1], Charles A. Odame-Ankrah[1], Jennifer A. Huo[1], Robert McLaren[2], Alex K. Y. Lee[3, 4],

5   Max G. Adam[4], Megan D. Willis[5], Jonathan P. D. Abbatt[5], Cristian Mihele[6], Andrea Darlington[6],

6   Richard L. Mittermeier[6], Kevin Strawbridge[6], Katherine L. Hayden[6], Jason S. Olfert[7], Elijah. G. Schnitzler[8],

7   Duncan K. Brownsey[1], Faisal V. Assad[1], Gregory R. Wentworth[5, a], Alex G. Tevlin[5], Douglas E. J. Worthy[6],

8   Shao-Meng Li[6], John Liggio[6], Jeffrey R. Brook[6], and Hans D. Osthoff[1*]

9

10   [1] Department of Chemistry, University of Calgary, Calgary, Alberta, T2N 1N4, Canada

11   [2] Centre for Atmospheric Chemistry, York University, Toronto, Ontario, M3J 1P3, Canada

12   [3] Department of Civil and Environmental Engineering, National University of Singapore, Singapore

13   117576, Singapore

14   [4] NUS Environmental Research Institute, National University of Singapore, Singapore

15   [5] Department of Chemistry, University of Toronto, Toronto, Ontario, M5S 3H6, Canada

16   [6] Air Quality Research Division, Environment and Climate Change Canada, Toronto, Ontario, M3H 5T4,

17   Canada

18   [7] Department of Mechanical Engineering, University of Alberta, Edmonton, Alberta, T6G 1H9, Canada

19   [8] Department of Chemistry, University of Alberta, Edmonton, Alberta, T6G 2G2, Canada

20   [a] Now at: Environmental Monitoring and Science Division, Alberta Environment and Parks, Edmonton,

21   Alberta, T5J 5C6, Canada

22   * Corresponding author

23

24

Atmospheric
Chemistry
and Physics
Discussions

25   **Abstract**

26   In this paper, measurements of air pollutants made at a ground site near Fort McKay in the Athabasca

27   oil sands region as part of a multi-platform campaign in the summer of 2013 are presented. The

28   observations included measurements of selected volatile organic compounds (VOCs) by a gas

29   chromatograph – ion trap mass spectrometer (GC-ITMS). This instrument observed a large, analytically

30   unresolved hydrocarbon peak (with retention index between 1100 and 1700) associated with

31   intermediate volatility organic compounds (IVOCs). However, the activities or processes that contribute

32   to the release of these IVOCs in the oil sands region remain unclear.

33   Principal component analysis (PCA) with Varimax rotation was applied to elucidate major source types

34   impacting the sampling site in the summer of 2013. The analysis included 28 variables, including

35   concentrations of total odd nitrogen (NO_y), carbon dioxide (CO_2), methane (CH_4), ammonia (NH_3), carbon

36   monoxide (CO), sulfur dioxide (SO_2), total reduced sulfur compounds (TRS), speciated monoterpenes

37   (including α- and β-pinene and limonene), particle volume calculated from measured size distributions

38   of particles less than 10 μm and 1 μm in diameter (PM_{10-1} and PM_1), particle-surface bound polycyclic

39   aromatic hydrocarbons (pPAH), and aerosol mass spectrometer composition measurements, including

40   refractory black carbon (rBC) and organic aerosol components. The PCA was complemented by bivariate

41   polar plots showing the joint wind speed and direction dependence of air pollutant concentrations to

42   illustrate the spatial distribution of sources in the area. Using the 95% cumulative percentage of

43   variance criterion, ten components were identified and categorized by source type. These included

44   emissions by wet tailings ponds, vegetation, open pit mining operations, upgrader facilities, and surface

45   dust. Three components correlated with IVOCs, with the largest associated with surface mining and is

46   likely caused by the unearthing and processing of raw bitumen.

Atmospheric
Chemistry
and Physics
Discussions

1. Introduction

The Athabasca oil sands region of Northern Alberta, Canada, has seen extraordinary expansion of its oil sands production and processing facilities (CAPP, 2016) and associated emissions of air pollutants over the last several decades (Englander et al., 2013; Bari and Kindzierski, 2015). Air emissions from these facilities have been impacting surrounding communities, including the city of Ft. McMurray and the community of Ft. McKay (WBEA, 2013). To assess the impact of these emissions on human health, visibility and climate, and the ecosystems downwind, it is critical to obtain an understanding of the source types from all activities associated with oil sands operations (ECCC, 2016).

Prior to 2013, there had been only a single industry-independent study of trace gas emissions from the Athabasca oil sands mining operations (Simpson et al., 2010; Howell et al., 2014). The data showed elevated concentrations in n-alkanes (30% of the total quantified hydrocarbon emissions), cycloalkanes (49%), and aromatics (15%) in plumes from an oil sands surface mining facility intercepted from a single aircraft flight. These compounds are associated with oil and gas developments including mining, upgrading, and transportation of bitumen (Siddique et al., 2006). Specifically, these activities involve the use of naphtha, a complex mixture of aliphatic and aromatic hydrocarbons in the range of C_3 to C_{14} containing n-alkanes (e.g., n-heptane, n-octane, and n-nonane) and benzene, toluene, ethylbenzene, and xylenes (BTEX).

In August 2013, a comprehensive air quality study as a part of the Joint Oil Sands Monitoring (JOSM) plan (JOSM, 2012), referred to here as the 2013 JOSM intensive study was conducted. This study was performed in northern Alberta at two ground sites in and near Fort McKay and from a National Research Council of Canada (NRC) Convair 580 research aircraft to characterize oil sands emissions and their downwind physical and chemical transformations (Gordon et al., 2015; Liggio et al., 2016; Li et al., 2017).

One ground site, located at the Wood Buffalo Environmental Association (WBEA) air monitoring station

Atmospheric
Chemistry
and Physics
Discussions

70   (AMS) 13 (Fig. 1), was equipped with a comprehensive set of instrumentation to measure

71   concentrations of trace gases and aerosols (Table 1). As part of this effort, a gas chromatograph

72   equipped with an ion trap mass spectrometer (GC-ITMS) was deployed at AMS 13. When air masses

73   passing over regions with industrial activities were observed (as judged from a combination of local wind

74   direction and tracer measurements), the total ion chromatogram showed an analytically unresolved

75   hydrocarbon signal associated with intermediate volatile organic compounds (IVOCs) with saturation

76   concentration (C^*) in the range 10^5 μg m^{-3}< C^* < 10^7 μg m^{-3} (Liggio et al., 2016).

77   Emission estimates for analytically unresolved hydrocarbons range from 5×10^6 kg year^{-1} to 14×10^6 kg

78   year^{-1} for the two facilities that reported such emissions (Li et al., 2017). Using aircraft measurements

79   during the 2013 study, Liggio et al. (2016) showed that IVOCs contributed to the majority of the

80   observed secondary organic aerosol (SOA) mass production in a similar fashion as anthropogenic VOCs

81   contributed to SOA production during the Deepwater Horizon oil spill (de Gouw et al., 2011) and rivaling

82   the magnitude of SOA formation observed downwind of megacities (Liggio et al., 2016), though

83   ultimately it has remained unclear which activities are associated with IVOC emissions.

84   In this paper, concurrent measurements of air pollutants at the AMS 13 ground site during the 2013

85   JOSM intensive study are presented and analyzed using principal component analysis (PCA) to elucidate

86   the origin of the IVOCs in the Athabasca oil sands. The analysis presented here is a receptor analysis

87   focusing on the normalized variability of pollutants impacting the AMS 13 ground site and hence does

88   not constitute a comprehensive emission profile analysis of the oil sands facilities as a whole, for which

89   aircraft-based measurements and/or direct plume or stack measurements are more suitable. The PCA

90   was complemented by bivariate polar plots (Carslaw and Ropkins, 2012; Carslaw and Beevers, 2013) to

91   show the spatial distribution of sources in the region as a function of locally measured wind direction

92   and speed. A second PCA was performed to investigate which components correlate with (and generate)

93   secondary pollutants, i.e., pollutants that are formed by atmospheric processes. Potential sources and

Atmospheric
Chemistry
and Physics
Discussions

94   processes contributing to each of the components identified by PCA are discussed.

95

96   **2. Experimental**

97   **2.1 Measurement location**

98   Measurements of air pollutants were made at AMS 13 routine air monitoring station (Fig. 1), which is

99   operated by WBEA. The site is located at 111.6423° W longitude and 57.1492° N latitude about 3 km

100   from the southern edge of the community of Fort McKay, 300 m west from a public road, and 1 km west

101   of the Athabasca river. The immediate vicinity of the site consisted of mixed-leaf boreal forest with a

102   variety of tree species, including poplar, aspen, pine and spruce trees (Smreciu et al., 2013). The site was

103   accessible via a gravel road; traffic on this road was restricted during the study period (August -

104   September, 2013).

105   The site is impacted by emissions from nearby oil sands facilities (Table 1 and Fig. 1), including a large

106   surface mining site operated by Syncrude Canada whose northeastern corner is located 3.5 km to the

107   south of AMS 13 (and which is adjacent to the 5 km long Syncrude – Mildred Lake (SML) tailings pond)

108   and from a large upgrader stack facility operated by Suncor Energy Inc. located to the Southeast. There

109   are additional oil sands facilities operated (during the study period) by Canadian Natural Resources

110   Limited, Imperial Oil, and Shell Canada to the North and Northeast.
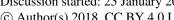
Atmospheric
Chemistry
and Physics
Discussions

111   **Table 1**. Oil sands facilities located within 30 km of AMS 13. Distances were estimated using coordinates

112   provided in the National Pollutant Release Inventory (NPRI, 2013) and do not account for the size of

113   each facility whose boundaries may be considerably closer to (or further away from) AMS 13. PACPRM =

114   Petroleum and coal products refining and manufacturing; OGPS = Oil and gas pipelines and storage.

Company	Name	Type	Direction	Distance (km)
Syncrude Canada Ltd.	Mildred Lake Plant Site	PACPRM	S	12.2
Athabasca Minerals Inc.	Susan Lake Gravel Pit	Mining and Quarrying	N	15.5
Syncrude Canada Ltd.	Aurora North Mine Site	PACPRM	NE	18.7
Suncor Energy	Suncor Energy Inc. Oil Sands	PACPRM	SE	19.4
Enbridge Pipelines Inc.	MacKay River Terminal	OGPS	WSW	19.7
Suncor Energy	MacKay River, In-Situ, Oil Sands Plant	PACPRM	WSW	19.9
Enbridge Pipelines Inc.	Athabasca Terminal	OGPS	SE	21.2
Williams Energy	Fort McMurray Hydrocarbon Liquids Extraction Facility	Conventional oil and gas extraction	SE	21.6
Canadian Natural Resources Limited	Horizon Oil Sands Processing Plant and Mine	PACPRM	NNW	21.8
Shell Canada Energy	Muskeg River Mine and Jackpine Mine	PACPRM	NNE	23.7

115

116

Atmospheric
Chemistry
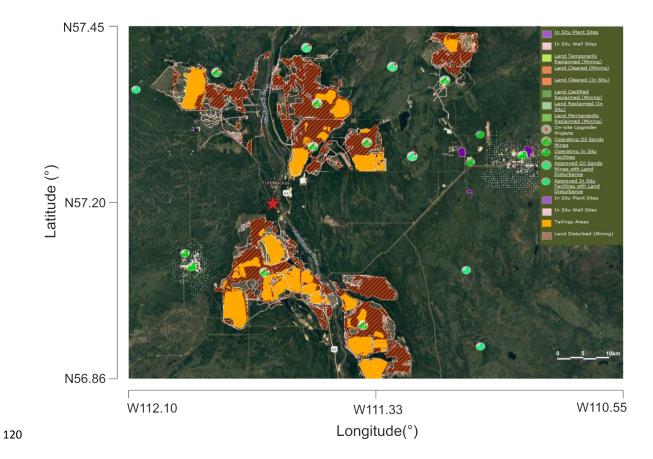and Physics
Discussions

117

118   **Figure 1**. Map of oil sands facilities showing locations of surface mines and tailings ponds, downloaded

119   from the Oil Sands Information Portal (Alberta, 2017). The red star indicates the location of AMS 13.

120

121   **2.2 Instrumentation**

122   A large number of instruments was deployed for this study; a partial list whose data were utilized in this

123   manuscript is given in Table 2. A detailed description of these instruments is given in the S.I. Sample

124   observations of analytically unresolved hydrocarbons by GC-ITMS and how these data were used in the

125   analysis are described in section 2.2.1 below.

Atmospheric
Chemistry
and Physics
Discussions

126   **Table 2**. Instruments used to measure ambient gas-phase and aerosol species during the 2013 JOSM

127   intensive study at AMS 13.

Instrument and Model	Species measured	Operated by	Reference
Picarro CRDS G2401	CO, CO_2, CH_4	York University and ECCC	(Chen et al., 2013; Nara et al., 2012)
Thermo Scientific, Model 42i	NO_y	University of Calgary	(Tokarek et al., 2014; Odame-Ankrah, 2015)
Blue diode cavity ring-down spectroscopy	NO_2	University of Calgary	(Paul and Osthoff, 2010; Odame-Ankrah, 2015)
Thermo Scientific Model 49i	O_3	University of Calgary	(Tokarek et al., 2014; Odame-Ankrah, 2015)
Griffin/FLIR, model 450 GC-ITMS	VOCs	University of Calgary	(Tokarek et al., 2017; Liggio et al., 2016)
Thermo Scientific CON101	TS	ECCC	n/a
Thermo Scientific 43iTLE	SO_2	ECCC	n/a
AIM-IC	$NH_{3(g)}$, $NH_4^+{}_{(p)}$	University of Toronto	(Markovic et al., 2012)
Aerodyne SP-AMS	rBC, $NH_4^+{}_{(p)}$, $SO_4^{2-}{}_{(p)}$, $NO_3^-{}_{(p)}$, $Cl^-{}_{(p)}$, organics	University of Toronto and ECCC	(Onasch et al., 2012)
TSI APS 3321	PM_{10-1} size distribution	University of Calgary	(Peters and Leith, 2003)
TSI SMPS (3081 DMA, 3776 CPC)	PM_1 size distribution	University of Alberta	(Wang and Flagan, 1990)
EcoChem Analytics PAS 2000CE	pPAH	ECCC	(Wilson et al., 1994; Burtscher et al., 1982)

128

Atmospheric
Chemistry
and Physics
Discussions

129   **2.2.1 Analytically unresolved hydrocarbon signature**

130   As previously reported (Liggio et al., 2016), the total ion chromatogram of the GC-ITMS occasionally

131   showed elevated and analytically unresolved hydrocarbons in the volatility range of $C_{11} - C_{17}$ with

132   saturation vapor concentration (C^*) from 10^5 µg m^{-3}< C^* < 10^7 µg m^{-3}. An example is shown in Fig. 2.
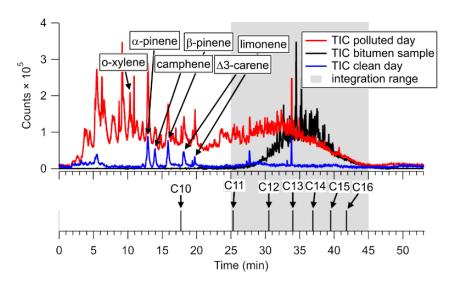

133

134   **Figure 2. (Top)** Total ion chromatograms of air samples collected on August 27, 2013 from 18:04 to

135   18:14 UTC (red) and on August 28, 2013 from 13:43 to 13:53 UTC (blue). The TIC of a head space sample

136   of ground-up bitumen collected post-campaign is superimposed (black). The gray area indicates the

137   range over which IVOC signal was integrated. **(Bottom)** Retention times of n-alkanes.

138

139   This unresolved signal was integrated in all ambient air chromatograms from a retention time of 25 min

140   to 45 min (gray area in Fig. 2). A qualitatively similar unresolved signal was observed in an offline

141   analysis of the headspace above ground-up bitumen (Fig. 2, black trace). In this particular case, the

142   ambient air chromatogram also shows enhancements of lower molecular weight hydrocarbons (possibly

143   from naphtha) that were not observed in the bitumen sample.

Atmospheric
Chemistry
and Physics
Discussions

144

145   **2.3 Principal Component Analysis**

146   The PCA was carried out using the "Statistical Analysis System" (SAS™) Studio 3.4 software (SAS, 2015)

147   using a method similar to that described by Thurston et al. (2011; 1985). The source-related

148   components and their associated profiles are derived from the correlation matrix of the input trace

149   constituents. This approach assumes that the total concentration of each "observable" (i.e., input

150   variable) is made up of the sum of contributions from each of a smaller number of pollution sources and

151   that variables are conserved between the points of emission and observation.

152   **2.3.1 Selection of variables**

153   22 variables whose ambient concentrations are dominated by primary emissions or which are formed

154   very shortly after emission (such as the less oxidized oxygenated organic aerosol (LO-OOA) factor

155   observed by the SP-AMS, see below) were included in the PCA (Table 3). These variables included CO_2,

156   CH_4, NO_y, CO, and SO_2, which are known to be emitted in the oil sands region from stacks, the mine fleet

157   and faces, tailings ponds, and by fugitive emissions (Percy, 2013). The median NO_x (= NO + NO_2) to NO_y

158   ratio was 0.85, consistent with the close proximity of the measurement site to emission sources and

159   limited chemical processing. Because NO_x constituted a large fraction of NO_y, its temporal variation was

160   captured by the latter, and it was not included as a separate variable in the PCA analysis.

161   For this work, mixing ratios of all non-methane hydrocarbons (NMHCs) that were quantified (i.e., o-

162   xylene, the n-alkanes decane and undecane, the aromatics 1, 2, 3- and 1, 2, 4-TMB, as well as limonene

163   and α- and β-pinene) were included as variables. In addition, the aforementioned unresolved signal

164   associated with IVOCs was included as a variable by integrating total GC-ITMS ion counts (*m/z* 50 –425)

165   over a retention time range of 25-45 min (retention index range of 1100 to 1700).

Atmospheric
Chemistry
and Physics
Discussions

166   Gas-phase ammonia was included as a variable because elevated reduced nitrogen concentrations have

167   been observed in the region and were linked to the use of ammonia on an industrial scale, for example

168   as a floating agent and for hydrotreating (Bytnerowicz et al., 2010). Total sulfur and total reduced sulfur

169   were added as tracers of upgrader stack SO_2 emissions and of "odours", believed to be emitted from oil

170   sands tailings ponds which continue to be of concern in surrounding communities (Small et al., 2015;

171   Percy, 2013; Holowenko et al., 2000).

172   Refractory black carbon was added as a variable since it is present in Diesel truck exhaust and in biomass

173   burning plumes and, hence, a combustion tracer (Wang et al., 2016; Briggs and Long). pPAHs were

174   included because of their association with facility stack emissions and combustion particles in the area

175   (Allen, 2008; Grimmer et al., 1987). Hydrocarbon-like organic aerosol (HOA) was included as a surrogate

176   for fossil fuel combustion by vehicles (Jimenez et al., 2009). The LO-OOA factor was included as it is

177   unique to the Alberta oil sands and appears to form rapidly after emission of precursors (Lee et al., In

178   prep). Supermicron aerosol volume (PM_{10-1}, i.e., the volume of particles between PM_{10} and PM_1) was

179   also included as a tracer of coarse particles from primary sources, which are expected to be dominated

180   by dust emissions.

181

Atmospheric
Chemistry
and Physics
Discussions

182   **Table 3.** Variables observed at the AMS 13 ground site during the 2013 JOSM campaign used for PCA.

Variable	Unit	Median[a]	Average[a,b]	Standard deviation[a,b]	LOD[e]	Min.[a]	Max.[a]
Anthropogenic VOCs							
o-xylene	pptv[f]	5	30	69	1	< LOD	635
1,2,3 - TMB	pptv	1.7	4.3	7.9	0.2	< LOD	67
1,2,4 - TMB	pptv	2.1	7.7	14.7	0.2	< LOD	107
decane	pptv	0.5	8.5	18.2	0.1	< LOD	125
undecane	pptv	0.4	3.0	6.3	0.1	< LOD	37
Biogenic VOCs							
α-pinene	pptv	477	542	401	1	19	1916
ß-pinene	pptv	390	467	334	1	18	1594
limonene	pptv	150	179	158	2	< LOD	711
Combustion tracers							
NO_y	ppbv	1.79	4.00	5.44	0.01	0.13	41.6
rBC	µg m^{-3}	0.13	0.20	0.10	0.02	< LOD	0.90
CO	ppbv	117.6	120.0	18.2	5.7[h]	90.9	241.2
CO_2	ppmv	420.2	433.2	39.5	0.4[h]	386.0	577.7
Aerosol species							
pPAH	ng m^{-3}	1	2	2	1[c]	< LOD	14
PM$_{10-1}$	µm^3 cm^{-3}	11.2	14.4	12.9	0.003	1.0	79.5
HOA	µg m^{-3}	0.31	0.43	0.35	N/A[g]	0.04	2.32
LO-OOA	µg m^{-3}	1.19	2.00	2.26	N/A[g]	0.11	15.6
Sulfur species							
Total sulfur (TS)	ppbv	0.22	1.41	4.27	0.13	< LOD	33.3
SO_2	ppbv	< LOD	1.0	4.0	0.2	< LOD	33.5
Total reduced sulfur (TRS)	ppbv	0.26	0.38	1.05	0.2	< LOD	14.8
Other							
IVOCs	Counts × min	1.8×10^7	3.4×10^7	4.2×10^7	N/A[g]	1.4×10^6	2.5×10^8
CH_4	ppbv	1999.2	2065.5	169.6	1.8[h]	1880	2959
NH_3	µg m^{-3}	0.79	1.10	1.03	0.05	0.06	5.75

[a] Values were determined only from data points included in PCA analysis, not from entire campaign.
[b] Average and standard deviation were calculated before zeros were replaced with 0.5×LOD.
[c] Estimated.
[e] LOD = limit of detection.
[f] parts-per-trillion by volume (10^{-12})
[g] N/A = data not available
[h] calculated using 3 × standard deviation at ambient background levels

183

Atmospheric
Chemistry
and Physics
Discussions

Open Access
EGU

184   To assess which components have the greatest impact on secondary product formation, a second PCA

185   was performed which included variables mainly formed through atmospheric chemical processes and

186   whose concentrations more strongly depend on air mass chemical age than those variables selected

187   initially. In this PCA, odd oxygen ($O_x = O_3 + NO_2$), submicron aerosol $SO_4^{2-}{}_{(p)}$, $NO_3^-{}_{(p)}$, $NH_4^+{}_{(p)}$, a second,

188   more-oxidized OOA factor (MO-OOA), and PM_1 volume were included, increasing the total number of

189   variables to 28 (Table 4).

190

191   **Table 4.** Variables added in the second PCA. Particle-phase concentrations, i.e., $SO_4^{2-}{}_{(p)}$, $NO_3^-{}_{(p)}$, $NH_4^+{}_{(p)}$

192   and MO-OOA were made by aerosol mass spectrometry and account for PM_1 only.

Variable	Unit	Median	Average	Standard deviation	LOD	Min.	Max.
O_x	ppbv	7.35	11.1	10.6	1	<LOD	41.1
$SO_4^{2-}{}_{(p)}$	µg m^{-3}	0.3	0.8	1.1	0.1	<LOD	6.6
$NO_3^-{}_{(p)}$	µg m^{-3}	0.08	0.13	0.13	0.01	0.01	0.72
$NH_4^+{}_{(p)}$	µg m^{-3}	0.13	0.28	0.37	0.05	<LOD	2.21
MO-OOA	µg m^{-3}	1.65	1.83	0.960	N/A	1.41×10^{-6}	4.65
PM_1 volume	µm^3 cm^{-3}	2.48	3.77	3.72	N/A	0.35	20.9

193

Atmospheric
Chemistry
and Physics
Discussions
Open Access

194   **2.3.2 Treatment of input data**

195   Data used in the PCA analysis were averaged to match the time resolution of the GC-ITMS VOC and IVOC

196   measurements, i.e. over 10 minute long periods (spaced ~ 1 hr apart) set by the start and stop times of

197   the GC-ITMS pre-concentration period. When concentrations were below their respective limit of

198   detection (LOD; values are given in Table 3), half the reported LOD was used to minimize bias (Harrison

199   et al., 1996; Buhamra et al., 1998). Prior to PCA, input variables were standardized to eliminate unit

200   differences by subtracting the mean concentration $\overline{C_i}$ of pollutant i from the concentration of sample k

201   ($C_{i,k}$) and dividing by the standard deviation (s_i) of all samples included in the PCA analysis.

202    $$Z_{i,k} = \frac{C_{i,k} - \overline{C_i}}{s_i}$$ (1)

203   Here, $Z_{i,k}$ is the standardized pollutant concentration. In total, 218 data points from all identified species

204   over the period of the campaign were used for the main PCA analysis.

205

206   **2.3.3 PCA solutions**

207   In this work, the Varimax method (Kaiser, 1958) was used to rotate the loading matrix. This method is an

208   orthogonal rotation (i.e., components are not expected to correlate) which minimizes the impact of high

209   loadings, making the results easier to interpret (Kaiser, 1958). Several criteria (Table S-10) were

210   considered for component selection: the latent root criterion, i.e., on the basis that rotated eigenvalues

211   must be greater than unity, the (cumulative) percentage of variance criterion, where the extracted

212   components accounts for >95% of the variance, and the Scree test (Fig. S-1) (Thurston and Spengler,

213   1985; Guo et al., 2004; Hair et al., 1998; Cattell, 1966). For the optimal solution presented in the main

214   manuscript, the 95% variance criterion was chosen, providing a 10-component solution for the PCA with

215   only primary variables and an 11-component solution for the PCA with both primary and secondary

216   variables. Solutions with fewer and more components are presented in the supplemental material

217   section.

218   Time series of each of the components were calculated by multiplying the original standardized matrix

219   by the rotated loading matrix and were used to generate bivariate polar plots (section 2.4).

220

221   **2.4 Bivariate polar plots**

222   The PCA was complemented by bivariate polar plots showing the wind speed and direction dependence

223   of air pollutant concentrations. The use of these representations implies a linear relationship between

224   local wind conditions and air mass origin, which may not be always the case (for example, during or after

225   stagnation periods). In addition, local topography, such as the Athabasca river valley, complicates

226   regional air flow patterns and limit the interpretability of polar plots in general and in particular to the E

227   of AMS 13, where the river valley is located. The plots were generated with the Openair software

228   package (Carslaw and Ropkins, 2012; Carslaw and Beevers, 2013) using the R programming language and

229   the open-source software "RStudio: Integrated development environment for R" (RStudio Boston,

230   2017). The default setting (100) was used as the smoothing function.

231   **3. Results**

232   **3.1. Overview of the data set**

233   Time series of the 22 pollution tracers chosen for PCA analysis are presented in Fig. 2, grouped

234   approximately by source type. Statistics of the data (i.e., median, average, maxima, minima, etc.) are

235   summarized in Table 3.

236

Atmospheric
Chemistry
and Physics
Discussions

Open Access

237

Figure 3. Time series of selected pollution tracers observed at the AMS 13 ground site in the Athabasca

oil sands during the 2013 JOSM measurement intensive. The gray and yellow backgrounds represent

night and day, respectively. (**A**) Selected non-methane hydrocarbons (NMHCs) and IVOCs. (**B**)

Combustion product tracers: refractory black carbon (rBC), total odd nitrogen (NO_y) and particle surface

bound polycyclic aromatic hydrocarbons (pPAH), and organic aerosol components: hydrocarbon-like

organic aerosol (HOA) and less oxidized oxygenated organic aerosol (LO-OOA). (**C**) Methane (CH_4),

carbon dioxide (CO_2) and monoxide (CO). (**D**) Total sulfur (TS), sulfur dioxide (SO_2), and total reduced

sulfur (TRS) and PM_{10} particle volume. (**E**) Biogenic VOCs (α-pinene, ß-pinene and limonene) and

ammonia (NH_3).

Atmospheric
Chemistry
and Physics
Discussions

247   Time series of VOCs of primarily anthropogenic origin (i.e., o-xylene, 1, 2, 3- and 1, 2, 4-TMB, etc.) as

248   well as the IVOC signature are shown in Fig. 3A. The abundances of these species, as well as the other

249   compounds, were highly variable and varied as a function of time of day (i.e., boundary layer mixing

250   height) and air mass origin, with higher VOC concentrations generally observed during daytime. The VOC

251   concentrations varied between nearly pristine, remote conditions, with concentrations below

252   detectable limits, to mixing ratios of aromatic species exceeding 100 pptv. The concentration range of o-

253   xylene is within the extremes reported by WBEA in their 2013 annual report (WBEA, 2013), exemplifying

254   that the data set is representative of typical pollutant levels in this region.

255   While there is some obvious covariance between variables (i.e., when the mixing ratios of one particular

256   VOC increases, so do others), the ratios of hydrocarbons varied considerably. For example, on August

257   18, 10:50 UTC, the n-decane to o-xylene ratio was ~22:1, whereas on August 24, 07:40 UTC it was ~1:5.7.

258   The IVOC magnitude also varied greatly and often increased and decreased in tandem with the other

259   VOCs (e.g., on Aug 24, 16:30 UTC) but also increased independently from the other VOC abundances

260   (e.g., on Aug 30, 01:20 UTC, and on the night of Aug 22). This behaviour suggests the presence of

261   multiple sources with distinct signatures that are being sampled to a varying extent at different times.

262   This, coupled with the intermittency of the highly elevated signals, presents an analysis problem

263   frequently encountered in environmental analysis that is usually investigated through a factor or

264   principal component analysis (Thurston et al., 2011; Guo et al., 2004).

265   Presented in Fig. 3B are the time series of NO_y, rBC and pPAH abundances, all of which are combustion

266   byproducts. For example, rBC is emitted from combustion of fossil fuels, biofuels, open biomass burning,

267   and burning of urban waste (Bond et al., 2004). Similar to the VOCs, the abundances of these species

268   varied greatly, from very low, continental background levels (i.e., <100 pptv of NO_y, < LOD for rBC and

269   pPAHs) to polluted concentrations (i.e., > 60 ppbv of NO_y, > 1 µg m^{-3} rBC, > 10 ng m^{-3} pPAHs)

270   characteristic of polluted urban and industrial areas. When high concentrations of NO_y were observed,

Atmospheric
Chemistry
and Physics
Discussions

271   its main component was NO_x (data not shown), which is a combustion byproduct usually associated with

272   automobile exhaust. In the Alberta oil sands, emissions from off-road mining trucks as well as the

273   upgrading processes are the main contributors to the NO_y burden (Percy, 2013; Watson et al., 2013).

274   Shown in Fig. 3C are the mixing ratios of the greenhouse gases CH_4 and CO_2 along with CO. Abundances

275   of CO_2 were clearly attenuated by photosynthesis and respiration of the vegetation near the

276   measurement site, as judged from the strong diurnal cycle in its concentration (not shown). Maxima

277   typically occurred shortly after sunrise, coincident with the expected break-up of the nocturnal

278   boundary layer. In addition to biogenic emissions from vegetation and soil, CO_2 originates from a variety

279   of point and mobile sources in this region, including off-road mining trucks (Watson et al., 2013) and the

280   extraction, upgrading, and refining of bitumen and on-road vehicle sources in the area (Nimana et al.,

281   2015a, b). Concentrations of CO_2 spiked whenever these emissions were transported to the

282   measurement site.

283   Concentrations of CH_4 also exhibit a diurnal cycle, with higher concentrations generally observed at

284   night and peaking in the early morning hours. While CH_4 and CO_2 mixing ratios frequently correlated in

285   plumes, their ratios were variable overall, suggesting they originated from distinct sources. Potential

286   methane point sources in the region include microbial production in tailings ponds (Siddique et al.,

287   2012) and fugitive emissions associated with the mining and processing of bitumen (Johnson et al.,

288   2016). Indeed, a recent analysis shows tailings ponds and open pit mining sources to be the largest

289   sources of CH_4 in the region (Baray et al., submitted, 2017).

290   Similar to the anthropogenic VOCs, the abundances of CH_4 and CO_2 were highly variable and ranged

291   from minima of 1.88 and 384 ppmv to maxima of 2.96 and 578 ppmv, corresponding to maximum

292   enhancements of 1.63 and 1.47 relative to tropospheric global monthly means of 1.806±0.001 and

293   394.3±0.1 ppmv for July, 2013 (Dlugokencky, 2017b, a), respectively.

Atmospheric
Chemistry
and Physics
Discussions

294   Mixing ratios of CO also varied with time but generally were not elevated greatly (median 118 ppbv)

295   above background levels (minimum 91 ppbv), except for occasional spikes in concentration (Fig. 3C).

296   Carbon monoxide is a tracer of biomass burning and fossil fuel combustion, in particular in automobiles

297   with poorly performing or absent catalytic converters, but is also a byproduct of the oxidation of VOCs,

298   in particular of methane and isoprene which are oxidized over a wide area upwind of AMS 13 (Miller et

299   al., 2008).

300   Time series of sulfur species and PM_{10-1} volume are shown in Fig. 3D. The TS and SO_2 data are dominated

301   by intermittent plumes containing SO_2 mixing ratios exceeding 5 ppbv. The highest mixing ratio

302   observed was 92.5 ppbv (in between the preconcentration periods of the GC-ITMS). Mixing ratios of SO_2

303   exhibited the most variability of all pollutants, as judged from the standard deviation of each of the

304   measurements (Table 3). TRS levels were generally small (< 1 ppbv) and variable, except for plumes; TRS

305   abundances in plumes, however, are more uncertain since they were calculated by subtraction of two

306   large numbers. When TS and SO_2 abundances were low (< 1 ppbv), TRS abundances were variable and

307   occasionally exhibited spikes that did not show any obvious correlation with other variables, suggesting

308   the presence of one or more distinct TRS sources. PM_{10} volume concentrations varied a lot as well and,

309   just like TRS, did not show an obvious correlation with other variables. Fugitive dust emissions likely

310   contributed to much of the PM_{10} volume in the Athabasca oil sands region (Wang et al., 2015).

311   Time series of monoterpene mixing ratios are shown in Fig. 3E. α-Pinene was generally the most

312   abundant monoterpene, followed by β-pinene. Their ratio, averaged over the entire campaign was

313   1:0.85, though occasionally the α- to β-pinene ratio was below 1:2 (e.g., on Aug 28, 14:50 UTC and Sept

314   5, 12:40 UTC). Terpene mixing ratios were generally higher at night than during the day, with maxima of

315   1.9 and 1.6 ppbv, respectively, a diurnal pattern consistent with what has been observed at other forest

316   locations (Fuentes et al., 1996). Monoterpenes are emitted by plants via both photosynthetic and non-

317   photosynthetic pathways (Fares et al., 2013; Guenther et al., 2012); at night, their emissions accumulate

Atmospheric
Chemistry
and Physics
Discussions

318   in a shallow nocturnal boundary layer, whereas during daytime, they are entrained aloft (above the

319   canopy) and oxidized by the hydroxyl radical (OH) and O_3, which are more abundant during the day than

320   at night (Fuentes et al., 1996). α- and β-pinene mixing ratios were lowest mid-day (median values at

321   noon of 140 and 133 pptv, respectively). The largest daytime concentrations were observed on Aug 25, a

322   cloudy day (as judged from spectral radiometer measurements of the NO_2 photolysis frequency): on this

323   particular day, mixing ratios at noon were 687 and 850 pptv, respectively.

324   Also shown in Fig. 3E is the time series of ammonia. These data were dominated by spikes which were

325   observed sporadically and did not correlate with other variables, suggesting the presence of nearby

326   ammonia point sources. Ammonia was not as variable as some of the other pollutants (e.g., the

327   anthropogenic VOCs, sulfur species) as judged from its standard deviation (Table 3), which suggests a

328   geographically more disperse source or sources similar to CO or CH_4, which have a "background". This is

329   consistent with a recent study by Whaley et al. (2017) that estimated over half (~57%) of the near-

330   surface NH_3 during the study period originated from NH_3 bi-directional exchange (i.e. re-emission of NH_3

331   from plants and soils), with the remainder being from a mix of anthropogenic sources (~20%) and forest

332   fires (~23%).

333

334   **3.2. Principal component analysis**

335   **3.2.1. PCA analysis with primary variables**

336   The loadings of the optimum solution are presented in Table 5. The 10-component solution accounts for

337   a cumulative variance of 95.5%. The communalities for the analysis, i.e., the fraction of total pollutant

338   observations accounted for by the PCA are all greater than 85%, with the lowest communality obtained

339   for the IVOCs (0.86).

340   In the following, an overview of the observed components is presented. Associations with r>0.7, r>0.3,

Atmospheric
Chemistry
and Physics
Discussions

341   and r>0.1 are referred to as "strong", "moderate", and "weak", respectively. Hypothesized

342   identifications are given in section 4 and are summarized in Table 6 and Fig. 4.

343   The component accounting for most of the variance of the data, component 1, is strongly associated

344   with the anthropogenic VOCs (r > 0.87), moderately associated with CH_4 (r = 0.59), TRS (r = 0.59), HOA (r

345   = 0.40), LO-OOA (r = 0.45), CO (r = 0.41), and the IVOCs (r = 0.31), and weakly associated with NO_y (r =

346   0.27) and rBC (r = 0.30). Component 2 is strongly associated with the combustion tracers NO_y (r = 0.82),

347   rBC (r = 0.77), HOA (r = 0.74), and pPAH (r = 0.94), moderately associated with CH_4 (r = 0.39) and IVOCs (r

348   = 0.39), and weakly associated with ammonia (r = 0.20), CO (r = 0.18) and undecane and decane (r = 0.27

349   and 0.22, respectively). Component 3 is strongly associated (r > 0.9) with the biogenic VOCs and

350   moderately associated with CO_2 (r = 0.48) and shows weak negative correlations with NO_y (r = -0.26),

351   ammonia (r = -0.24), and SO_2 (r = -0.15). Component 4 is strongly associated with SO_2 and TS (r = 0.97

352   and 0.93, respectively) and weakly with NO_y (r = 0.21) and LO-OOA (r = 0.28).

353   Components 1 through 4 emerged regardless of the number of components used to represent the data,

354   whereas the structure of components 5 through 10 only fully emerged in the 10-component solution

355   (see S.I.). Hence, components 6 through 10 are somewhat tentative as many (i.e., 7 – 9) are single

356   variable components and have eigenvalues close to or below unity, i.e., account for less variance than

357   any single variable. For the purpose of this manuscript, this is inconsequential as components 6 – 10 are

358   not associated with IVOCs.

359

Atmospheric
Chemistry
and Physics
Discussions

360   **Table 5.** Loadings for the 10-factor, optimal solution (primary variables only). Coefficients with Pearson

361   correlation coefficients r>0.3 are interpreted as being moderately or strongly associated with a

362   component and are shown in bold font.

	1	2	3	4	5	6	7	8	9	10	Commu-nalities
Anthropogenic VOCs											
o-xylene	**0.88**	0.08	0.02	0.10	0.14	0.13	0.07	-0.04	0.16	**0.32**	0.95
1,2,3 - TMB	**0.93**	0.16	0.07	0.05	0.05	0.11	0.04	-0.02	0.18	-0.01	0.95
1,2,4 - TMB	**0.94**	0.14	0.01	0.10	0.11	0.08	0.07	-0.03	0.18	0.13	0.98
decane	**0.92**	0.22	-0.02	0.15	0.23	0.01	0.05	0.04	0.04	0.03	0.97
undecane	**0.87**	0.27	-0.08	0.23	0.20	-0.06	0.12	0.07	-0.04	-0.10	0.96
Biogenic VOCs											
α-pinene	-0.03	-0.08	**0.98**	-0.11	0.02	0.04	0.01	-0.08	0.02	0.01	0.98
ß-pinene	-0.02	-0.08	**0.98**	-0.12	0.02	0.03	0.02	-0.07	0.00	0.01	0.98
limonene	0.07	-0.03	**0.92**	-0.08	0.12	0.24	0.05	-0.11	0.03	-0.05	0.95
Combustion tracers											
NO_y	0.27	**0.82**	-0.26	0.21	0.22	-0.04	0.02	0.10	-0.08	0.01	0.92
rBC	**0.30**	**0.77**	0.03	0.05	**0.44**	0.10	0.09	0.13	0.12	-0.10	0.94
CO	**0.41**	0.18	0.04	0.02	0.09	0.09	0.08	0.06	**0.87**	-0.01	0.99
CO_2	0.09	0.08	**0.48**	-0.12	-0.03	**0.77**	0.25	-0.14	0.05	-0.08	0.95
Aerosol species											
pPAH	0.06	**0.94**	-0.07	-0.13	-0.11	0.07	0.01	0.13	0.10	0.04	0.95
PM_{10-1}	0.18	0.14	0.08	0.09	0.11	0.17	**0.93**	-0.03	0.07	0.08	0.98
HOA	**0.40**	**0.74**	0.02	0.12	0.25	0.15	0.23	-0.06	0.16	0.09	0.90
LO-OOA	**0.45**	0.11	0.12	0.28	**0.72**	0.05	0.25	0.00	0.10	0.04	0.91
Sulfur											
TS	0.25	0.04	-0.16	**0.93**	0.08	-0.05	0.07	-0.02	0.01	0.12	1.00
SO_2	0.12	0.03	-0.15	**0.97**	0.02	-0.04	0.03	-0.03	0.01	-0.05	0.99
TRS	**0.59**	0.04	-0.08	0.11	0.26	-0.04	0.16	0.04	-0.04	**0.71**	0.96
Other											
IVOCs	**0.31**	**0.39**	0.12	-0.08	**0.74**	-0.02	-0.02	-0.06	0.02	0.20	0.86
NH_3	0.01	0.20	-0.24	-0.05	-0.02	-0.08	-0.03	**0.94**	0.04	0.02	0.99
CH_4	**0.59**	**0.39**	0.10	-0.05	0.12	**0.59**	0.11	0.00	0.17	0.14	0.93
Eigenvalues	5.72	3.32	3.23	2.16	1.64	1.13	1.13	0.99	0.96	0.74	
% of variance	25.99	15.08	14.69	9.80	7.46	5.14	5.13	4.51	4.36	3.35	
Cumulative variance	25.99	41.07	55.76	65.56	73.02	78.16	83.30	87.81	92.17	95.52	

363

Atmospheric
Chemistry
and Physics
Discussions

364 **Table 6**. Hypothesized identification of principal components.

Component	Key observations	Possible source(s)	Relevant references
1	Enhancements of aromatics, n-alkanes, TRS, NO_y, rBC, HOA, LO-OOA, CO and CH_4	Wet tailings ponds and associated facilities	(Simpson et al., 2010; Small et al., 2015; Percy, 2013; Holowenko et al., 2000; Howell et al., 2014)
2	Enhancements of NO_y, rBC, pPAH and HOA due to engine exhaust	Mine fleet and operations	(Wang et al., 2016; Grimmer et al., 1987; Allen, 2008; Briggs and Long, 2016)
3	Enhancements of monoterpenes and CO_2, weak anticorrelation with NO_y and absence of anthropogenic VOCs	Biogenic emission and respiration	(Guenther et al., 2012; Helmig et al., 1999)
4	Enhancements of SO_2 and TS, weak correlation with NO_y and LO-OOA	Upgrader facilities	(Simpson et al., 2010; Kindzierski and Ranganathan, 2006)
5	Enhancements of IVOCs, rBC, LO-OOA, NO_y, and TRS	Surface exposed bitumen and hot-water based bitumen extraction	this work
6	Enhancements of CO_2 and CH_4, absence of combustion tracers	Mine face and soil	(Johnson et al., 2016; Rooney et al., 2012)
7	Enhancement of PM_{10-1}	Wind-blown dust	(Wang et al., 2015)
8	Enhancement of ammonia	Fugitive emissions from storage tanks and natural soil/plant emissions	(Bytnerowicz et al., 2010; Whaley et al., 2017)
9	Enhancement of CO	VOC oxidation	(Marey et al., 2015)
10	Enhancements of TRS and o-xylene, weak association with CH_4	Composite tailings	(Small et al., 2015; Warren et al., 2016)

365

366

Figure 4. Images of likely sources associated with each of the principal components. From top left to bottom: **(A)** Wet tailings ponds (component 1). **(B)** Mine truck fleet and highway traffic emissions (component 2). **(C)** Biogenic emissions from vegetation (component 3). **(D)** Upgrader facilities (component 4). **(E)** Exposed bitumen on mined surfaces (component 5). **(F)** Fugitive greenhouse gas emissions from mine faces (component 6). **(G)** Wind-blown dust from exposed sand (component 7). **(H)** Fugitive emissions of ammonia from storage tanks (Component 8). **(I)** Composite (dry) tailings (component 10). No image is shown for production CO from oxidation of VOCs (component 9).

374

375   **3.2.2. Extended PCA analysis with added secondary variables**

376   The loadings of the optimum solution that includes primary and secondary variables are shown in Table

377   7. In this 11-component solution, the 10 components originally identified were preserved, though their

378   relative order was changed, with the upgrader component moving from the 4th to 2nd position. There

379   was one new component (#6), which encompassed only secondary species, including MO-OOA (r =

380   0.92), O_x (r = 0.33), $NO_{3(p)}^-$ (r = 0.36), PM_1 (r = 0.31) and LO-OOA (r = 0.31).

381     $NH_{4(p)}^+$, $SO_{4(p)}^{2-}$, and $NO_{3(p)}^-$ are associated with the stack emissions component (#2, with r = 0.84, 0.84

382   and 0.44, respectively), which also moderately correlated with PM_1 (r = 0.44) and O_x (r = 0.36). The

383   association of secondary variables with the primary components suggests rapid formation of these

384   secondary products on a time scale that is similar to the transit time of the pollutants to the

385   measurement site. PM_1 and O_x correlated strongly with the major IVOC component (component 5, r =

386   0.80), which also moderately associated with LO-OOA (r=0.66) and $NO_{3(p)}^-$ (r = 0.59), as well as $NH_{4(p)}^+$

387   and $SO_{4(p)}^{2-}$ (r = 0.32 and 0.33, respectively).

388

Atmospheric
Chemistry
and Physics
Discussions

389   **Table 7.** Loadings for the 11-component solution with the inclusion of variables associated with

390   secondary processes.

	1	2	3	4	5	6	7	8	9	10	11	Commu-nalities
Anthropogenic VOCs												
o-xylene	**0.89**	0.16	0.04	0.04	0.15	0.00	0.10	0.07	-0.04	0.17	0.24	0.94
1,2,3 - TMB	**0.91**	0.13	0.10	0.16	0.09	0.07	0.11	0.03	-0.03	0.16	-0.08	0.95
1,2,4 - TMB	**0.93**	0.19	0.02	0.13	0.13	0.05	0.06	0.07	-0.03	0.17	0.06	0.99
decane	**0.89**	0.25	0.00	0.22	0.26	0.05	-0.01	0.05	0.01	0.00	0.01	0.98
undecane	**0.81**	**0.35**	-0.08	0.27	0.21	0.15	-0.07	0.08	0.04	-0.12	-0.10	0.96
Biogenic VOCs												
α-pinene	0.00	-0.08	**0.98**	-0.07	0.05	0.03	0.01	0.01	-0.07	0.02	0.01	0.98
ß-pinene	0.01	-0.08	**0.98**	-0.08	0.05	0.05	0.01	0.03	-0.06	0.01	0.02	0.98
limonene	0.11	-0.02	**0.92**	-0.02	0.14	0.09	0.21	0.02	-0.10	0.02	-0.03	0.95
Combustion tracers												
NO_y	0.23	0.20	-0.27	**0.82**	0.21	-0.06	-0.07	0.03	0.10	-0.10	0.01	0.92
rBC	0.22	0.15	0.05	**0.80**	**0.43**	0.15	0.10	0.05	0.09	0.07	0.00	0.95
CO	**0.40**	0.09	0.08	0.20	0.09	0.22	0.08	0.06	0.03	**0.83**	-0.02	0.97
CO_2	0.12	-0.07	**0.50**	0.08	-0.03	0.09	**0.75**	0.28	-0.12	0.03	-0.08	0.95
Aerosol species												
pPAH	0.06	-0.10	-0.06	**0.93**	-0.07	-0.06	0.07	0.03	0.15	0.13	-0.05	0.94
PM_{10-1}	0.19	0.16	0.08	0.16	0.13	0.08	0.18	**0.91**	-0.03	0.05	0.07	0.99
PM_1	0.24	**0.44**	0.00	0.17	**0.70**	0.31	-0.06	0.11	-0.04	0.07	-0.14	0.90
$NH_4^+{}_{(p)}$	0.28	**0.84**	0.02	0.12	**0.32**	0.22	0.06	0.07	-0.04	0.14	-0.04	0.97
$SO_4^{2-}{}_{(p)}$	0.29	**0.84**	0.03	0.12	**0.33**	0.19	0.06	0.06	-0.05	0.12	-0.05	0.97
$NO_3^-{}_{(p)}$	**0.30**	**0.44**	0.09	0.23	**0.59**	**0.36**	0.08	0.15	-0.13	0.02	0.24	0.92
HOA	**0.37**	0.18	0.02	**0.77**	0.25	0.10	0.10	0.18	-0.08	0.13	0.14	0.93
LO-OOA	**0.37**	**0.40**	0.12	0.16	**0.66**	0.31	0.03	0.12	-0.06	0.00	0.27	0.97
MO-OOA	0.10	0.15	0.09	0.00	0.10	**0.92**	0.05	0.07	0.10	0.16	-0.03	0.95
Sulfur												
TS	0.27	**0.90**	-0.20	0.03	0.04	-0.04	-0.09	0.07	0.00	-0.04	0.18	0.98
SO_2	0.09	**0.96**	-0.19	0.02	-0.03	-0.01	-0.08	0.03	-0.02	-0.03	0.00	0.98
TRS	**0.65**	0.14	-0.10	0.05	0.23	-0.08	-0.07	0.17	0.06	-0.04	**0.63**	0.95
Other												
IVOCs	**0.34**	-0.01	0.12	**0.33**	**0.80**	-0.23	-0.02	0.02	0.02	0.06	0.06	0.94
NH_3	-0.03	-0.08	-0.22	0.21	-0.04	0.09	-0.07	-0.03	**0.93**	0.02	0.02	0.99
O_x	0.07	**0.36**	**-0.62**	0.01	0.27	**0.33**	**-0.41**	-0.07	-0.03	-0.14	0.12	0.91
CH_4	**0.60**	0.00	0.14	**0.42**	0.10	0.08	**0.57**	0.08	-0.04	0.13	0.16	0.94
Eigenvalues	5.85	4.30	3.71	3.51	2.78	1.58	1.24	1.09	1.01	0.94	0.75	
% of variance	20.90	15.34	13.25	12.52	9.92	5.65	4.43	3.88	3.59	3.37	2.66	
Cumulative variance	20.90	36.24	49.49	62.02	71.94	77.59	82.03	85.90	89.50	92.87	95.53	

Atmospheric
Chemistry
and Physics
Discussions

3.3 Spatial distribution of IVOC sources

Bivariate polar plots were generated for all components and their dominant, associated variables and

are shown in the supplemental material section (Figs. S2-S11). Winds were predominantly from the SW

but were also observed often from the S and N. Fig. 5A shows the plot for IVOCs. The highest

concentrations were observed when the local wind direction was from the NE, where several facilities

including the Aurora North, Musket River and Jackpine mines and large swaths of disturbed and cleared

land are located in close proximity to each other (Table 1 and Fig. 1). The second highest IVOC signal

intensity was observed when local wind direction was from the SSE.

The bivariate polar plots of the 3 components associated with IVOCs are shown in Fig. 5B-D. These

components are associated with winds from the NE, E, SE and S at low to moderate speeds (1-3 m s^{-1}).

Component 5 (Fig. 5B) was the most strongly correlated with IVOCs and shows the most spatial overlap

with the distribution of the IVOC source; however, the intensities differ owing to the association of

component 5 with other variables such rBC and LO-OOA.

404

Figure 5. Bivariate polar plots related to IVOCs: **(A)** IVOCs from the complete data set. **(B)** Component 5

405

extracted from the main PCA (Table 5). **(C)** Component 1 extracted from the main PCA. **(D)** Component 2

406

extracted from the main PCA analysis. Wind direction is binned into 10° intervals and wind direction into

407

30° intervals. The polar axis indicates wind speed (m s^{-1}). a.u. = arbitrary units.

408

Atmospheric
Chemistry
and Physics
Discussions

4. Discussion

409

410 The main objective of this work is to elucidate the origin of the IVOC signature observed at the AMS 13

411 ground site downwind from the AB oil sands mining operations (Fig. 2) through a principal component

412 analysis. The optimum PCA solution identified 10 components, of which three were associated with the

413 IVOC signature: 1, 2, and 5 (Table 5). The assignments of these components to source types in the oil

414 sands are given in Table 6 and are discussed below.

415 Emission inventories show that the facilities that process the mined bitumen are by far the largest

416 anthropogenic point sources in the oil sands region (NPRI, 2013), consistent with recent aircraft

417 measurements (Howell et al., 2014; Li et al., 2017; Baray et al., submitted, 2017; Simpson et al., 2010)

418 which have shown substantial emissions of NO_y, SO_2, CO, VOCs, CO_2, and CH_4, from these facilities and

419 associated mining activities. No single component correlates with all of these variables, suggesting that

420 the PCA is able to distinguish between source types within the facilities such as tailings ponds

421 (component 1), stack emissions (component 4), and mining (component 2).

422 Close-up overflights (Howell et al., 2014; Li et al., 2017; Baray et al., submitted, 2017) were able to

423 spatially resolve various oil sands facility emission sources (i.e., tailings ponds from upgraders, fluid

424 coking reactors, hydrocrackers and –treaters); the PCA presented in this manuscript is not expected to

425 do this in all cases because some emissions would have frequently merged into a single plume by the

426 time of observation at AMS 13; unless their emissions vary considerably in time, these sources could be

427 interpreted as originating from a single source in the PCA.

428 The discussion below focuses on components that are associated with IVOCs (section 4.1), followed by

429 those that are not (section 4.2). The PCA analysis that included 6 secondary products is discussed in

430 section 4.3. Components which are not associated with IVOCs and have only tentatively been identified

431 (i.e., components 6 – 10) are discussed in the S.I.

4.1 Sources associated with IVOCs

4.1.1. Component 1: Tailings ponds (wet tailings)

Component 1 is strongly associated with anthropogenic VOCs (r > 0.87) and moderately with TRS (r = 0.59), and CH_4 (r = 0.59). These pollutants originate from tailings ponds (Small et al., 2015), though it is unclear from this analysis how large a source tailings ponds are compared to fugitive emissions of these pollutants from the nearby processing (e.g., bitumen separation and mining) facilities.

Tailings ponds cover large areas of land and are used to slowly (on a time scale of years to decades) separate solid components, or tailings, from water used in bitumen extraction. Residual bitumen often floats to the top of the settling basins. Most tailings ponds are "wet" (as they contain residual naphtha that is used as a diluent during the transfer of tailings to the ponds) and emit VOCs, CH_4, and CO_2 (Small et al., 2015). The presence of o-xylene, TMB and the n-alkanes in component 1 is consistent with the fugitive release of VOCs from residual naphtha, which contains these compounds (Siddique et al., 2008; Siddique et al., 2011; Small et al., 2015). Furthermore, the observation of TRS and CH_4 from this source is consistent with the presence of anaerobic sulfur reducing bacteria and methanogens within the ponds, which degrade not only the residual bitumen (Holowenko et al., 2000; Percy, 2013; Quagraine et al., 2005) but also the various components of naphtha (Shahimin and Siddique, 2017; Small et al., 2015). Overall, tailings ponds emissions explain much of the TRS and CH_4 concentration variability in this data set (Table 5) and in a recent aircraft study (Baray et al., submitted, 2017).

While component 1 correlates with CH_4 (r = 0.59), it does not correlate with CO_2 (r = 0.09). Emissions of CH_4 from tailings ponds due to methanogenic bacterial activity are well-documented (Small et al., 2015; Yeh et al., 2010) and hence the correlation with CH_4 is not unexpected. On the other hand, the lack of correlation with CO_2 seems inconsistent with emission inventories that generally present tailings ponds as large CO_2 sources (Small et al., 2015). One plausible explanation is that tailings ponds are a relatively

Atmospheric
Chemistry
and Physics
Discussions

455   small CO_2 source overall in the region and that other, larger CO_2 sources and sinks (such as

456   photosynthesis and respiration by the vegetation surrounding the site) dominate the variance impacting

457   the PCA results. It may also indicate that, at least on aggregate and for the particular ponds detected in

458   this work, the emissions are in a regime where the release of CH_4 dominates over CO_2, i.e., the ponds

459   have, perhaps, become more anoxic than believed to be the case in previous studies and hence emit

460   more CH_4 (Holowenko et al., 2000). For example, Small et al. (2015) showed that older tailings ponds

461   (those without the addition of fresh froth or thickening treatments) tended to emit more CH_4, while

462   newer ponds are associated with higher VOC emissions. It is likely that component 1 is dominated by the

463   nearest pond (the Mildred Lake settling basin, $6 - 11$ km SSE of AMS 13) and other tailings in the SE

464   where the majority of air samples originated from. The Mildred Lake settling basin is one of the oldest in

465   the region and is still actively being used; the correlation with CH_4 and VOC emissions is hence expected.

466   Component 1 is also associated with NO_y, rBC, CO, and HOA, though these correlations are relatively

467   modest (r = 0.27, 0.30, 0.41, and 0.40, respectively). These species typically originate from combustion

468   sources, such as generators, motor vehicles, including Diesel powered engines powering generators or

469   pumps; it is not obvious if and to what extent these are operated on or near tailings ponds, though.

470   Satellite observations have shown elevated concentrations of NO_2 above on-site upgrader facilities,

471   likely a result of emissions from extraction and transport sources (McLinden et al., 2012). In addition,

472   one of the major highways of the region is located adjacent to the Mildred Lake settling basin and other

473   major ponds in the region; highway traffic emissions (of CO, NO_y, rBC, and HOA) may hence also be

474   partially included in component 1.

475   The bivariate polar plot shows that component 1 was observed when local wind speeds were from the

476   SE and E of the measurement site (Fig. 5C), which is consistent with the notion that the Mildred Lake

477   settling basin and emissions along Highway 63 and, potentially, more distant facilities are sources

478   contributing to this component.

Atmospheric
Chemistry
and Physics
Discussions

Open Access

EGU

479   Component 1 is associated with the IVOC signature, though to a lesser degree than components 2 and 5.

480   The association of the IVOC signal with component 1 is slightly weaker (r = 0.31) than the association

481   with component 2 (r = 0.39), but significantly weaker than component 5 (r = 0.74). The association of

482   IVOCs with tailings ponds vapor can be explained by the presence of bitumen in the ponds that was not

483   separated from the sand during the separation stage (Holowenko et al., 2000). Tailings ponds contain

484   anywhere from 0.5% - 5% residual bitumen by weight (Chalaturnyk et al., 2002; Holowenko et al., 2000;

485   Penner and Foght, 2010). As illustrated in Fig. 4A, some of this material floats on the ponds' surfaces,

486   where IVOCs can partition to the air. Emission of IVOCs from bitumen floating on tailings ponds would

487   be a function of many variables (e.g., diluent composition, extraction methodology, settling rate,

488   temperature, etc.) and is thus not expected to be as persistent as CH_4 partitioning from the ponds to the

489   above air or from exposed bitumen on the mine surface, leading to a lower overall correlation.

490   Component 1 is also associated with the less oxidized oxygenated organic aerosol factor, LO-OOA (r =

491   0.45). Liggio et al. (2016) found that the observed secondary organic aerosol is dominated by an OOA

492   factor whose mass spectrum was similar to those of aerosols formed from oxidized bitumen vapours.

493   The organic aerosol budget in this study was also dominated by an OOA factor, the LO-OOA (Lee et al.,

494   In prep). The association of LO-OOA with component 1 is thus consistent with its association with IVOCs.

495   **4.1.2. Component 2: Mine fleet and vehicle emissions**

496   Component 2 strongly correlates with NO_y (r = 0.82), rBC (r = 0.77), pPAH (r = 0.94), and HOA (r = 0.74),

497   which suggests a combustion source such as Diesel engines. In the AB oil sands, there is a sizeable off-

498   road mining truck fleet consisting of heavy aggregate haulers. In addition, there are Diesel engine

499   sources associated with generators, pumps and land moving equipment, i.e., graders, dozers, hydraulic

500   excavators, and electric rope shovels (Watson et al., 2013; Wang et al., 2016). Most of these non-road

501   applications have been exempt from highway fuel taxes, on-road fuel formulation requirements and

502   after-engine exhaust treatment (Watson et al., 2013). Emissions from the hauler fleet and the stationary

503   sources would fit the profile of component 2. Other Diesel engines operated in the region include a

504   commuter bus fleet, pickup and delivery trucks, tractor-trailers, and privately owned Diesel powered

505   automobiles used to commute from the work sites to the major residential areas around Fort

506   McMurray, whose emissions are likely captured by component 2 as well, though the magnitude of these

507   relative to the mining truck fleet is not known. Consistent with component 2 being associated with an

508   anthropogenic source is its weak correlation with undecane (r =0.27), likely arising from fugitive fuel

509   emissions.

510   The bivariate polar plot (Fig. 5D) for component 2 and NO_y in particular (Fig. S-3A) match the location of

511   Highway 63 which crosses the river to the SE of AMS 13 and bends to the E and is indicative of a line

512   source. At the same time, some of the largest mining operations in the region, the Susan Lake Gravel Pit,

513   Aurora North, Muskeg river, and Millennium mines are located to the NE and SE of AMS 13 as well. NO_y,

514   rBC, and HOA (Fig. S-3A, B and D) all appear to have dominating point sources to the S and E when wind

515   speeds are 1-2 m s^{-1}. These directions are the same as the Fort McKay industrial park to the E and the

516   Syncrude Mildred Lake facility parking lot to the S which would have a higher concentration of vehicles

517   emitting these pollutants in a smaller area, whose emissions would be in addition to those from

518   industrial activities.

519   Component 2 is associated with the IVOCs signature and CH_4 (both r = 0.39). The mining activities bring

520   bitumen to the surface; similar to what we had observed in lab experiments (Fig. 2, black trace), the

521   surface exposure of bitumen during mining and on-site processing is expected to be associated with

522   fugitive emissions of CH_4 (Johnson et al., 2016) and IVOCs.

523   Fine-fraction particle-surface bound PAHs (pPAH) are associated strongly with component 2, but no

524   other components. Measurements of individual PAHs in snow and moss downwind from the oil sands

525 facilities have identified multiple sources of PAHs in the Athabasca oil sands, which include wind-blown

526 petroleum coke dust (also referred to as petcoke for short), a carbonaceous residual product from the

527 upgrading of crude petroleum that is stockpiled on mine sites, and emissions from fine tailings, oil sands

528 ore, and naturally exposed bitumen (Zhang et al., 2016; Jautzy et al., 2015; Parajulee and Wania, 2014).

529 Given this diversity of known sources, the associations of PAHs with only a single component is

530 surprising, though indicates that emissions from the mining fleet (which would include Diesel and,

531 perhaps, wind-blown emissions from petcoke that is being transported) gave rise to most of the

532 variability in surface-bound PAH concentrations in this data set. The petcoke emissions identified in the

533 studies mentioned above are likely mainly associated with larger, supermicron sized particles, whose

534 PAH content would not be detected by the pPAH measurement in this data set.

535 Component 2 is not significantly associated with LO-OOA (r = 0.11), even though IVOCs are associated

536 with this component. This feature may indicate that the IVOCs emitted in component 2 are qualitatively

537 different from those emitted by components 1 and 5, in that they are less likely to yield organic aerosol

538 on the time scale of transport from emission to observation. One reason for the difference could be that

539 the bitumen that is transported by the mining fleet is relatively freshly exposed, whereas the IVOCs

540 released by bitumen in tailings ponds has been processed by microbes and that released by mine faces

541 (component 5) may have been photochemically oxidized to a greater extent and hence more prone to

542 rapid aerosol formation.

543 There is little to no association of component 2 with either CO or CO_2 (r = 0.18 and 0.08, respectively).

544 This is somewhat unexpected as the trucks are expected to release both (Wang et al., 2016) but could be

545 due to significantly larger CO_2 sources in the area dominating the observed CO_2 variability at AMS 13

546 (e.g., components 3 and 6).

547

4.1.3. Component 5: Surface-exposed bitumen and hot-water bitumen extraction

548

549   Component 5 correlates more strongly with the IVOCs (r = 0.74) than with any other component and

550   correlates strongly with LO-OOA (r = 0.72), moderately with rBC (r = 0.44), and weakly with HOA (r =

551   0.25), NO_y (r = 0.22), decane (r = 0.23), undecane (r = 0.20), and TRS (r = 0.26). We interpret this profile

552   as emissions from surface-exposed bitumen which outgases IVOCs.

553   One possibility is that these emissions occur on mine faces, where previously unexposed bitumen is

554   brought to the surface as a result of mining. Only a relatively small portion of the mine faces is actively

555   mined; those parts give rise to rBC and NO_y emissions from combustion engines in heavy haulers or

556   generators powering equipment. The weak association of component 5 with TRS could be due to sulfur

557   reducing bacteria found on the surface of bitumen. However, most of the variability of TRS at AMS 13 is

558   attributed to composite or "dry" tailings ponds given their more conducive environment to microbial

559   activity.

560   Component 5 does not correlate with CO_2 (r = -0.03) and only weakly with CH_4 (r = 0.12), which is

561   somewhat at odds with the notion of mine faces as the main source of IVOCs. The mine faces give rise to

562   substantial fugitive emissions of CO_2 and CH_4 (Johnson et al., 2016) – these emissions are likely captured

563   by component 6 in this analysis (see S.I.). It is unclear to what extent these greenhouse gases are

564   released relatively quickly from "hot spots" (i.e., from a small number of locations) through surface

565   cracks and fissures or by slow release from new material that is exposed and then releases greenhouse

566   gases during material handling, transport and processing (Johnson et al., 2016). IVOCs from surface-

567   exposed bitumen are likely released by the latter mechanism and are temperature-dependent. If the

568   mine faces are indeed the main IVOC source, the analysis results presented here suggest that the IVOCs

569   emissions from surface-exposed bitumen on mine faces are decoupled from CH_4 emissions in time and

570   appear as a distinct component and hence corroborate the "hot spots" or fast release hypothesis,

Atmospheric
Chemistry
and Physics
Discussions

571   though clearly, more work is needed to characterize greenhouse gas emissions from oil sands mine

572   faces.

573   The association of IVOCs with component 5 may also be a result of fugitive emissions during the hot

574   water-based extraction of bitumen sand slurries during the separation phase of bitumen treatment.

575   Generally, bitumen is extracted in a weak alkaline environment by aeration of the solution to optimize

576   the separation of sand and bitumen (Masliyah et al., 2004). Unrecovered bitumen and naphtha then end

577   up in tailings. The recovered bitumen and naphtha are moved to upgrader facilities where they undergo

578   further treatment (such as coking or hydrotreatment). The magnitude of fugitive emissions during these

579   downstream extraction processes could be large, considering the bitumen is heated and actively

580   aerated. Future work should investigate IVOC fluxes near extraction plants and on mine faces.

581   Finally, it is conceivable that a "natural" background of IVOCs exists in the region (since bitumen can be

582   found at or near the surface in many parts of the region); such a natural background would also be

583   included in component 5. However, this "natural" bitumen would have been exposed at the surface for

584   geological time scales and, unlike unexposed, buried bitumen, likely would have lost most of its volatile

585   content over that period. Furthermore, the mine faces occupy large swaths of land in the region (as

586   evident from satellite imagery). Thus, the IVOCs emissions are more likely due to anthropogenic activity

587   than due to a natural phenomenon.

588

589   **4.2. Sources not associated with IVOCs**

590   **4.2.1. Component 3: Biogenic emissions and respiration**

591   Component 3 is strongly correlated with the monoterpenes α-pinene (r = 0.98), ß-pinene (r = 0.98) and

592   limonene (r = 0.92) and is hence identified as a biogenic emissions source. This component is also

593   moderately associated with CO_2 (r = 0.48).

594   At AMS 13, CO_2 and the monoterpenes exhibit a very similar diurnal cycle: they are present in higher

595   concentrations during the night than during the day (Fig. 3) due to a decrease in the boundary layer

596   height (BLH) at night coupled with plant respiration of CO_2 and non-photochemical emission of

597   monoterpenes (Fares et al., 2013; Guenther et al., 2012). During the day, mixing ratios of CO_2 are lower

598   due to plant uptake and photosynthesis, and mixing ratios of terpenes are lower due to higher mixing

599   heights and vertical entrainment and due to oxidation by O_3 and OH (Fuentes et al., 1996). Hence, the

600   PCA gives a *positive* correlation of monoterpenes with CO_2 even though the physical processes,

601   photosynthesis and respiration, work in opposite direction.

602   The bivariate polar plots (Fig. S-4A-C) show that the monoterpenes and CO_2 were observed in highest

603   concentrations when the wind speeds were low (< 1 m s^{-1}), consistent with formation of a stable

604   nocturnal boundary layer.

605   To corroborate this interpretation, the PCA was repeated with BLH estimated by a light detection and

606   ranging (LIDAR) instrument (Strawbridge et al., in prep.) added as a variable (Table S-9 in the S.I.). Since

607   BLH is not "emitted" by any source, it appears as a single variable component (r = 0.90). The only other

608   component that BLH (anti)correlates with is the biogenic component 3 (r = -0.35).

609   The dominant monoterpene species observed was α-pinene, followed by ß-pinene and limonene,

610   though occasionally there was twice as much ß-pinene than α-pinene in the sampled air. Some

611   variability of this ratio is expected since emission factors vary considerably between tree species (Geron

612   et al., 2000) which are not homogeneously distributed throughout the region (e.g., Fig. S1 of Rooney et

613   al. (2012)).

614   Simpson et al. (2010) observed enhancements of α-pinene and, to a greater extent, β-pinene over the

615   oil sands (up to 217 pptv and 610 pptv) compared to background levels of 20±7 and 84±24 pptv,

Atmospheric
Chemistry
and Physics
Discussions

616   respectively, during mid-day overflights (which occurred between 11:00 and 13:00 local time). Similar

617   enhancements were also reported by Li et al. (2017) who observed emissions of biogenic hydrocarbons

618   in the four facilities sampled, three of which showed a higher β- than α-pinene concentration. The PCA

619   analysis (Table 5) showed no significant correlation of α- and β-pinene with any of the anthropogenic

620   sources, which implies that the biogenic source strength is simply too large for any anthropogenic

621   emissions of terpenes to be picked up in the analysis, especially considering that terpenes are relatively

622   short-lived.

623   The biogenic source shows weak anticorrelations with NO_y (r = -0.26), NH_3 (r = -0.24), and SO_2 (r = -0.15).

624   Many NO_y species (i.e., NO_2, HONO, peroxycarboxylic nitric anhydrides or PAN, and HNO_3) and SO_2

625   deposit to the forest canopy (Hsu et al., 2016; Min et al., 2014; Fenn et al., 2015); at night, when mixing

626   heights are lower, their concentrations are expected to decrease faster than during the day and are thus

627   out of phase with the CO_2 and terpene concentrations. In addition, there is a time-of-day observation

628   bias for SO_2 and, to lesser extent, NO_y, which are found in upgrader plumes (see 4.2.2.). The weak

629   anticorrelation with NH_3 likely arises because the NH_3 emissions from plants are mainly stomatal and

630   scale with temperature and are hence larger during the day than at night, anticorrelated with the

631   terpene source (Whaley et al., 2017).

632   **4.2.2 Component 4: Upgrader emissions**

633   Component 4 is strongly correlated with SO_2 (r = 0.97) and total sulfur (r = 0.93). By far the largest

634   source of SO_2 in the region are upgrader facilities, which emit as much as 6×10^7 kg annually according to

635   emission inventories (ECCC, 2013). Significant SO_2 emissions from upgrader facilities have recently been

636   confirmed by aircraft studies (Simpson et al., 2010; Howell et al., 2014; Liggio et al., 2016). Component 4

637   is also weakly correlated with NO_y (r = 0.21) but not with rBC (r = 0.05), consistent with a non-sooty (i.e.,

638   lean) combustion source such as upgrader stacks. Strong enhancements in SO_2 were only observed

639   intermittently as "spikes", which is expected when sampling emissions from relatively few and discrete

640   point sources.

641   Component 4 is weakly anticorrelated with CO_2 (r = -0.12), even though inventories indicate that the

642   upgrading facilities are the largest CO_2 source in the region (Furimsky, 2003; Englander et al., 2013; Yeh

643   et al., 2010). In this data set, the lack of correlation of component 4 with CO_2 (and to some extent with

644   PM_{10-1} as well) likely arises mainly from a sampling bias as stack emissions were only observed during

645   daytime, likely due to diurnal variability of the atmospheric boundary layer structure as explained

646   below.

647   Most of the variability in CO_2 concentration at AMS 13 is due to surface-based sources that originate

648   from large areas, especially biogenic processes (photosynthesis during the day and respiration at night,

649   component 3) and anthropogenic surface sources such as those captured by component 6 (section

650   4.2.3). Other anthropogenic pollutants, such as SO_2, NO_y, and CH_4, are not subject to large biogenically

651   driven processes and are less affected than CO_2.

652   In contrast to surface sources, emissions from the > 100 m tall stacks are comparatively under sampled

653   and observed mainly during daytime, when vertical mixing brings elevated plumes to the surface, yet

654   CO_2 concentrations are generally much lower than during the night due to uptake by vegetation. At

655   night, pollutants emitted from stacks are injected above the likely very shallow nocturnal surface layer

656   and were hence not observed at the surface. Vertical profile measurements of SO_2 stack plumes by a

657   Pandora spectral sun photometer at Fort McKay during daytime have shown considerable vertical

658   gradients and only occasional transport of SO_2 all the way to the surface (Fioletov et al., 2016).

659   The association of component 4 with CO_2 is negative because the stack emission source is observed only

660   during the day when the large biogenic sink dominates and effectively masks the relatively small

661   increase due to anthropogenic CO_2. In contrast, background concentrations of SO_2 are comparatively

Atmospheric
Chemistry
and Physics
Discussions

662   low, and the increase in SO_2 concentrations is readily picked up the PCA.

663   It would be interesting to conduct a future study in winter when biogenic activities decrease; a

664   wintertime PCA analysis of surface measurements might be able to associate CO_2 enhancements with

665   upgraders, though boundary layer mixing heights would decrease as well, which would make a PCA

666   analysis using surface data even more challenging.

667   Component 4 does not correlate with PM_{10-1} volume (r = 0.09). It is clear that the emitted SO_2 will

668   contribute to secondary aerosol formation downwind, such that a correlation of stack emissions with

669   PM_{10-1} volume might be expected. However, these secondary contributions will likely mostly be in the

670   submicron aerosol fraction, which adds relatively little to PM_{10-1} volume. Further, PM_{10-1} volume is

671   dominated by coarse particles from other primary sources, mostly wind-blown emission of sand from

672   the mine surfaces, roadways and, perhaps, bioaerosol (component 7, see S.I.). These effects make PM_{10-1}

673   volume from stacks appear comparatively small, such that the variability of the larger, surface-based

674   sources likely masks the contribution of stacks emissions to PM_{10-1} variability.

675   The bivariate polar plot of component 4 (Fig. S-5D) shows that the largest magnitudes were observed

676   when local winds were from the SE. The corresponding plot of SO_2 (Fig. S-5A) reveals two more distinct

677   sources: a larger one from the E and a smaller one from the SSE. However, only two facilities (Sunrise

678   and Firebag) are located to the E at relatively large distances of 37 km and 47 km respectively. The

679   largest known upgraders and SO_2 sources in the area (i.e., upgraders located at the Mildred Lake and

680   Suncor base plants) are located to the S and SE of AMS 13. Considering that the stack emissions are only

681   observed intermittently, we speculate that there exists a mesoscale transport pattern in the Athabasca

682   river valley which channel emissions, such that the local wind direction and speed may be misleading as

683   to the true location of these sources. For more extensive data sets, such phenomena may very well

684   average out but perhaps did not in this case.

4.3. Extended PCA with added secondary variables

685

686   The extended analysis (Table 7) qualitatively preserves the structure (with the exception of an added

687   "Aged" component, # 6) of the original 10-component solution but allows an assessment of which

688   components most result in formation of secondary products such as SOA, which has implications for

689   health (Bernstein, 2004) and climate (Charlson et al., 1992). Secondary products vary considerably as a

690   function of air mass chemical age (which depends, amongst other components, on time of day and

691   synoptic conditions, including wind speed) and are hence expected to add considerable noise and

692   scatter to the results leading to lower correlations. On the other hand, the distance between the

693   measurement site and sources is fixed, such that this variability should average out over time. This

694   indeed appears to have happened in this data set in spite of the relatively low sample size.

695   The analysis indicates that the strongest IVOC source (Component 5) has the largest impact on PM_1

696   (Table 7). Aircraft measurements combined with a modelling study have required a group of IVOC

697   hydrocarbons to explain the significant SOA formation and growth downwind of the oil sands region

698   (Liggio et al., 2016). The association of IVOCs with PM_1 volume is consistent with the hypothesis that

699   oxidation of IVOCs observed at AMS 13 leads to SOA generation and appears to have a significant impact

700   on the variation in PM_1 mass.

701   The second component influencing PM_1 is that from stack emissions (Component 4 in the primary PCA;

702   Component 2 in the secondary PCA) (Tables 5 and 7). It is well established that the oxidation of SO_2 to

703   sulfate will lead to formation of fine particulate matter. This apparently occurs, at least partially, on the

704   time scale between the point of emission and the AMS 13 site (assuming a wind speed of 3 m/s and a

705   distance of 11 km, the transit time is 1 hour), though some fraction of $SO_4^{2-}(p)$ is likely directly emitted.

Atmospheric
Chemistry
and Physics
Discussions

5. Summary and conclusions

706

707   A PCA was applied to continuous measurements of 22 primary pollutant tracers at the AMS 13 ground

708   site in the Athabasca oil sands during the 2013 JOSM intensive study to elucidate the origins of airborne

709   analytically unresolved hydrocarbons that were observed by GC-ITMS. The analysis identified 10

710   components. Three components correlated with the IVOC signature and were assigned to mine faces

711   and, potentially, hot-water bitumen extraction facilities, the mine hauler fleet, and wet tailings ponds

712   emissions. All three are anthropogenic activities that involve the handling of raw bitumen, i.e., the

713   unearthing, mining and transport of crude bitumen, and the disposal of processed material that contains

714   residual bitumen in wet tailings ponds. The PCA results are consistent with our previous interpretation

715   that the unresolved hydrocarbons originate from bitumen, which was based on the similarity of the

716   chromatograms with those obtained in a head space vapor analysis of ground-up bitumen in the

717   laboratory.

718   Liggio et al. (2016) showed that these hydrocarbons constitute a group of IVOCs in the saturation vapor

719   concentration (C^*) range 10^5 µg m^{-3}< C^* < 10^7 µg m^{-3} that contribute significantly to secondary organic

720   aerosol formation and growth downwind of the oil sands facilities. The correlation of LO-OOA with 2 of

721   the 3 IVOC components in the main PCA analysis and with PM$_1$ in the extended analysis corroborates the

722   high SOA formation potential of IVOCs and suggests that further differentiation may be needed and

723   stresses the need for IVOCs to be routinely monitored. In particular, direct measurements of emissions

724   throughout the processing of raw bitumen are needed to pinpoint source contributions more accurately

725   and aid in the development of potential mitigation strategies.

726   The PCA analysis in this study suffered from a several limitations. For instance, PCA does not provide

727   insight into the magnitudes of emissions, though it does capture what conditions change ambient

728   concentrations the most. Further, the receptor nature of PCA did not always discern between large

Atmospheric
Chemistry
and Physics
Discussions

729   source areas that may have many individual point sources coming together at the point of observation.

730   For example, component 1 contains an obvious tailings pond signature because of its high correlations

731   with anthropogenic VOCs, methane and TRS, but also includes several combustion sources, making

732   interpretation of this IVOC source location more challenging. A longer continuous data set with a greater

733   number of variables would have perhaps been able to resolve these different sources, including the

734   various tailings ponds, of which there are 19 in the region, all with slightly different emission profiles

735   (Small et al., 2015) .

736   Another limitation is the bias of this (and most) ground site data set towards surface-based emissions

737   and the undersampling of stack emissions. Facility stacks were only observed in the daytime because at

738   night the mixing height is so low that the stacks are emitting directly into the residual layer. These

739   emissions could be quantified using aircraft based platforms (Baray et al., submitted, 2017; Howell et al.,

740   2014; Li et al., 2017). The PCA struggled most with the allocation of greenhouse gases. Mixing ratios of

741   CO_2, in particular, were difficult to reconcile in this analysis due to a high background and large

742   attenuation by biogenic activity and boundary layer meteorology. Forests greatly affected CO_2 levels in

743   the region because it is taken up during the day when plants are photosynthetically active and emitted

744   at night when plants undergo cellular respiration. This CO_2 source and sink appears to dominate the

745   PCA, effectively masking relatively small emissions from tailings ponds, facilities, and tail pipes in

746   particular from the mine hauling fleet.

747   Finally, there is a need for improved monitoring methods for IVOCs. For instance, future studies should

748   focus on characterizing the VOCs in the above mentioned volatility range using a greater mass and time

749   resolution instrument, such as a time-of-flight mass spectrometer (TOF-MS) or higher resolution

750   separation methods (e.g., multi-dimensional gas chromatography).

Atmospheric
Chemistry
and Physics
Open Access
Discussions
EGU

Atmospheric
Chemistry
and Physics
Discussions

6. References

759   Government of Alberta, oil sands information portal: http://osip.alberta.ca, access: 23-FEB-2017, 2017.
760
761   Allen, E. W.: Process water treatment in Canada's oil sands industry: II. A review of emerging
762   technologies, J. Environ. Eng. Sci., 7, 499-524, 10.1139/s08-020, 2008.
763
764   Baray, S., Darlington, A., Gordon, M., Hayden, K. L., Li, S.-M., Liu, P. S. K., Mengistu, R., O'Brien, J.,
765   Staebler, R., Worthy, D., Moussa, S., and McLaren, R.: Identification and Quantification of Methane
766   Sources in the Athabasca Oil Sands Region of Alberta by Aircraft Mass-Balance, Atmos. Chem. Phys., acp-
767   2017-925, submitted, 2017.
768
769   Bari, M., and Kindzierski, W. B.: Fifteen-year trends in criteria air pollutants in oil sands communities of
770   Alberta, Canada, Environ. Int., 74, 200-208, 10.1016/j.envint.2014.10.009, 2015.
771
772   Bernstein, D. M.: Increased mortality in COPD among construction workers exposed to inorganic dust,
773   Eur. Resp. J., 24, 512-512, 10.1183/09031936.04.00044504, 2004.
774
775   Bond, T. C., Streets, D. G., Yarber, K. F., Nelson, S. M., Woo, J. H., and Klimont, Z.: A technology-based
776   global inventory of black and organic carbon emissions from combustion, J. Geophys. Res.-Atmos., 109,
777   1-43, 10.1029/2003JD003697, 2004.
778
779   Briggs, N. L., and Long, C. M.: Critical review of black carbon and elemental carbon source
780   apportionment in Europe and the United States, Atmos. Environ., 144, 409-427,
781   10.1016/j.atmosenv.2016.09.002, 2016.
782
783   Buhamra, S. S., Bouhamra, W. S., and Elkilani, A. S.: Assessment of air quality in ninety-nine residences of
784   Kuwait, Environ. Technol., 19, 357-367, 10.1080/09593331908616691, 1998.
785
786   Burtscher, H., Scherrer, L., Siegmann, H. C., Schmidtott, A., and Federer, B.: Probing aerosols by
787   photoelectric charging, J. Appl. Phys., 53, 3787-3791, 10.1063/1.331120, 1982.
788
789   Bytnerowicz, A., Fraczek, W., Schilling, S., and Alexander, D.: Spatial and temporal distribution of
790   ambient nitric acid and ammonia in the Athabasca Oil Sands Region, Alberta, J. Limnol., 69, 11-21,
791   10.3274/jl10-69-s1-03, 2010.
792
793   The facts on Canada's oil sands: http://www.capp.ca/publications-and-statistics/publications/296225,
794   access: April 20, 2017, 2016.
795
796   Carslaw, D. C., and Ropkins, K.: openair - An R package for air quality data analysis, Environ. Modell.
797   Softw., 27-28, 52-61, 10.1016/j.envsoft.2011.09.008, 2012.
798
799   Carslaw, D. C., and Beevers, S. D.: Characterising and understanding emission sources using bivariate
800   polar plots and k-means clustering, Environ. Modell. Softw., 40, 325-329, 10.1016/j.envsoft.2012.09.005,
801   2013.
802
803   Cattell, R. B.: The Scree Test For The Number Of Factors, Multivariate Behavioral Research, 1, 245-276,
804   10.1207/s15327906mbr0102_10, 1966.

Atmospheric
Chemistry
and Physics
Discussions

805

806   Chalaturnyk, R. J., Don Scott, J., and Ozum, B.: Management of oil sands tailings, Petroleum Science and
807   Technology, 20, 1025-1046, 10.1081/lft-120003695, 2002.
808
809   Charlson, R. J., Schwartz, S. E., Hales, J. M., Cess, R. D., Coakley, J. A., Hansen, J. E., and Hofmann, D. J.:
810   Climate forcing by anthropogenic aerosols, Science, 255, 423-430, 1992.
811
812   Chen, H., Karion, A., Rella, C. W., Winderlich, J., Gerbig, C., Filges, A., Newberger, T., Sweeney, C., and
813   Tans, P. P.: Accurate measurements of carbon monoxide in humid air using the cavity ring-down
814   spectroscopy (CRDS) technique, Atmos. Meas. Tech., 6, 1031-1040, 10.5194/amt-6-1031-2013, 2013.
815
816   de Gouw, J. A., Middlebrook, A. M., Warneke, C., Ahmadov, R., Atlas, E. L., Bahreini, R., Blake, D. R.,
817   Brock, C. A., Brioude, J., Fahey, D. W., Fehsenfeld, F. C., Holloway, J. S., Le Henaff, M., Lueb, R. A.,
818   McKeen, S. A., Meagher, J. F., Murphy, D. M., Paris, C., Parrish, D. D., Perring, A. E., Pollack, I. B.,
819   Ravishankara, A. R., Robinson, A. L., Ryerson, T. B., Schwarz, J. P., Spackman, J. R., Srinivasan, A., and
820   Watts, L. A.: Organic Aerosol Formation Downwind from the Deepwater Horizon Oil Spill, Science, 331,
821   1295-1299, 10.1126/science.1200320, 2011.
822
823   Trends in atmospheric methane: www.esrl.noaa.gov/gmd/ccgg/trends_ch4/, access: April 11, 2017,
824   2017a.
825
826   Trends in atmospheric carbon dioxide: www.esrl.noaa.gov/gmd/ccgg/trends/, access: April 11, 2017,
827   2017b.
828
829   National pollutant release inventory (NPRI): http://open.canada.ca/data/en/dataset/e40099ae-b116-
830   4c48-9475-f3806fe5a6a6, access: October 5, 2016, 2013.
831
832   ECCC: Joint oil sands monitoring program emissions inventory compilation report, Environment and
833   Climate Change Canada, Downsview, 2016.
834
835   Englander, J. G., Bharadwaj, S., and Brandt, A. R.: Historical trends in greenhouse gas emissions of the
836   Alberta oil sands (1970-2010), Environ. Res. Lett., 8, 10.1088/1748-9326/8/4/044036, 2013.
837
838   Fares, S., Schnitzhofer, R., Jiang, X., Guenther, A., Hansel, A., and Loreto, F.: Observations of Diurnal to
839   Weekly Variations of Monoterpene-Dominated Fluxes of Volatile Organic Compounds from
840   Mediterranean Forests: Implications for Regional Modeling, Environ. Sci. Technol., 47, 11073-11082,
841   10.1021/es4022156, 2013.
842
843   Fenn, M. E., Bytnerowicz, A., Schilling, S. L., and Ross, C. S.: Atmospheric deposition of nitrogen, sulfur
844   and base cations in jack pine stands in the Athabasca Oil Sands Region, Alberta, Canada, Environ. Pollut.,
845   196, 497-510, 10.1016/j.envpol.2014.08.023, 2015.
846
847   Fioletov, V. E., McLinden, C. A., Cede, A., Davies, J., Mihele, C., Netcheva, S., Li, S. M., and O'Brien, J.:
848   Sulfur dioxide (SO_2) vertical column density measurements by Pandora spectrometer over the Canadian
849   oil sands, Atmospheric Measurement Techniques, 9, 2961-2976, 10.5194/amt-9-2961-2016, 2016.
850

851 Fuentes, J. D., Wang, D., Neumann, H. H., Gillespie, T. J., DenHartog, G., and Dann, T. F.: Ambient
852 biogenic hydrocarbons and isoprene emissions from a mixed deciduous forest, J. Atmos. Chem., 25, 67-
853 95, 10.1007/BF00053286, 1996.
854
855 Furimsky, E.: Emissions of carbon dioxide from tar sands plants in Canada, Energy Fuels, 17, 1541-1548,
856 10.1021/ef0301102, 2003.
857
858 Geron, C., Rasmussen, R., Arnts, R. R., and Guenther, A.: A review and synthesis of monoterpene
859 speciation from forests in the United States, Atmos. Environ., 34, 1761-1781, 10.1016/S1352-
860 2310(99)00364-7, 2000.
861
862 Gordon, M., Li, S. M., Staebler, R., Darlington, A., Hayden, K., O'Brien, J., and Wolde, M.: Determining air
863 pollutant emission rates based on mass balance using airborne measurement data over the Alberta oil
864 sands operations, Atmos. Meas. Tech., 8, 3745-3765, 10.5194/amt-8-3745-2015, 2015.
865
866 Grimmer, G., Brune, H., Deutschwenzel, R., Dettbarn, G., Jacob, J., Naujack, K. W., Mohr, U., and Ernst,
867 H.: Contribution of polycyclic aromatic-hydrocarbons and nitro-derivatives to the carcinogenic impact of
868 diesel-engine exhaust condensate evaluated by implantation into the lungs of rats, Cancer Lett., 37, 173-
869 180, 10.1016/0304-3835(87)90160-1, 1987.
870
871 Guenther, A. B., Jiang, X., Heald, C. L., Sakulyanontvittaya, T., Duhl, T., Emmons, L. K., and Wang, X.: The
872 Model of Emissions of Gases and Aerosols from Nature version 2.1 (MEGAN2.1): an extended and
873 updated framework for modeling biogenic emissions, Geosci. Model Dev., 5, 1471-1492, 10.5194/gmd-
874 5-1471-2012, 2012.
875
876 Guo, H., Wang, T., and Louie, P. K. K.: Source apportionment of ambient non-methane hydrocarbons in
877 Hong Kong: Application of a principal component analysis/absolute principal component scores
878 (PCA/APCS) receptor model, Environ. Pollut., 129, 489-498, 10.1016/j.envpol.2003.11.006, 2004.
879
880 Hair, J. F., Anderson, R. E., Tatham, R. L., and Black, W. C.: Multivariate data analysis, in, 7th edition ed.,
881 Prentice-Hall, Upper Saddle River, NJ, pp. 108 -110, 1998.
882
883 Harrison, R. M., Smith, D. J. T., and Luhana, L.: Source apportionment of atmospheric polycyclic aromatic
884 hydrocarbons collected from an urban location in Birmingham, UK, Environ. Sci. Technol., 30, 825-832,
885 10.1021/es950252d, 1996.
886
887 Helmig, D., Klinger, L. F., Guenther, A., Vierling, L., Geron, C., and Zimmerman, P.: Biogenic volatile
888 organic compound emissions (BVOCs) I. Identifications from three continental sites in the U.S,
889 Chemosphere, 38, 2163-2187, 10.1016/S0045-6535(98)00425-1, 1999.
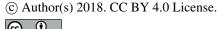890
891 Holowenko, F. M., MacKinnon, M. D., and Fedorak, P. M.: Methanogens and sulfate-reducing bacteria in
892 oil sands fine tailings waste, Canadian Journal of Microbiology, 46, 927-937, 10.1139/cjm-46-10-927,
893 2000.
894
895 Howell, S. G., Clarke, A. D., Freitag, S., McNaughton, C. S., Kapustin, V., Brekovskikh, V., Jimenez, J. L.,
896 and Cubison, M. J.: An airborne assessment of atmospheric particulate emissions from the processing of
897 Athabasca oil sands, Atmos. Chem. Phys., 14, 5073-5087, 10.5194/acp-14-5073-2014, 2014.
898

Atmospheric
Chemistry
and Physics
Discussions

899   Hsu, Y. M., Bytnerowicz, A., Fenn, M. E., and Percy, K. E.: Atmospheric dry deposition of sulfur and
900   nitrogen in the Athabasca Oil Sands Region, Alberta, Canada, Sci. Tot. Environm., 568, 285-295,
901   10.1016/j.scitotenv.2016.05.205, 2016.
902
903   Jautzy, J. J., Ahad, J. M. E., Gobeil, C., Smirnoff, A., Barst, B. D., and Savard, M. M.: Isotopic Evidence for
904   Oil Sands Petroleum Coke in the Peace-Athabasca Delta, Environm. Sci. Technol., 49, 12062-12070,
905   10.1021/acs.est.5b03232, 2015.
906
907   Jimenez, J. L., Canagaratna, M. R., Donahue, N. M., Prevot, A. S. H., Zhang, Q., Kroll, J. H., DeCarlo, P. F.,
908   Allan, J. D., Coe, H., Ng, N. L., Aiken, A. C., Docherty, K. S., Ulbrich, I. M., Grieshop, A. P., Robinson, A. L.,
909   Duplissy, J., Smith, J. D., Wilson, K. R., Lanz, V. A., Hueglin, C., Sun, Y. L., Tian, J., Laaksonen, A.,
910   Raatikainen, T., Rautiainen, J., Vaattovaara, P., Ehn, M., Kulmala, M., Tomlinson, J. M., Collins, D. R.,
911   Cubison, M. J., E., Dunlea, J., Huffman, J. A., Onasch, T. B., Alfarra, M. R., Williams, P. I., Bower, K.,
912   Kondo, Y., Schneider, J., Drewnick, F., Borrmann, S., Weimer, S., Demerjian, K., Salcedo, D., Cottrell, L.,
913   Griffin, R., Takami, A., Miyoshi, T., Hatakeyama, S., Shimono, A., Sun, J. Y., Zhang, Y. M., Dzepina, K.,
914   Kimmel, J. R., Sueper, D., Jayne, J. T., Herndon, S. C., Trimborn, A. M., Williams, L. R., Wood, E. C.,
915   Middlebrook, A. M., Kolb, C. E., Baltensperger, U., and Worsnop, D. R.: Evolution of Organic Aerosols in
916   the Atmosphere, Science, 326, 1525-1529, 10.1126/science.1180353, 2009.
917
918   Johnson, M. R., Crosland, B. M., McEwen, J. D., Hager, D. B., Armitage, J. R., Karimi-Golpayegani, M., and
919   Picard, D. J.: Estimating fugitive methane emissions from oil sands mining using extractive core samples,
920   Atmos. Environm., 144, 111-123, 10.1016/j.atmosenv.2016.08.073, 2016.
921
922   Kaiser, H. F.: The varimax criterion for analytic rotation in factor-analysis, Psychometrika, 23, 187-200,
923   10.1007/bf02289233, 1958.
924
925   Kindzierski, W. B., and Ranganathan, H. K. S.: Indoor and outdoor SO2 in a community near oil sand
926   extraction and production facilities in northern Alberta, J. Environ. Eng. Sci., 5, S121-S129, 10.1139/s06-
927   022, 2006.
928
929   Lee, A. K. Y., Adam, M. G., Willis, M. D., Abbatt, J. P. D., Tokarek, T. W., Odame-Ankrah, C. A., Huo, J. A.,
930   Osthoff, H. D., Li, S.-M., and Brook, J. R.: Large anthropogenic sources of organonitrate from Alberta oil
931   sands emissions, In prep.
932
933   Li, S.-M., Leithead, A., Moussa, S. G., Liggio, J., Moran, M. D., Wang, D., Hayden, K., Darlington, A.,
934   Gordon, M., Staebler, R., Makar, P. A., Stroud, C. A., McLaren, R., Liu, P. S. K., O'Brien, J., Mittermeier,
935   R. L., Zhang, J., Marson, G., Cober, S. G., Wolde, M., and Wentzell, J. J. B.: Differences between measured
936   and reported volatile organic compound emissions from oil sands facilities in Alberta, Canada,
937   Proceedings of the National Academy of Sciences, 114, E3756-E3765, 10.1073/pnas.1617862114, 2017.
938
939   Liggio, J., Li, S.-M., Hayden, K., Taha, Y. M., Stroud, C., Darlington, A., Drollette, B. D., Gordon, M., Lee, P.,
940   Liu, P., Leithead, A., Moussa, S. G., Wang, D., O'Brien, J., Mittermeier, R. L., Brook, J., Lu, G., Staebler, R.,
941   Han, Y., Tokarek, T. W., Osthoff, H. D., Makar, P. A., Zhang, J., Plata, D., and Gentner, D. R.: Oil Sands
942   Operations as a Large Source of Secondary Organic Aerosols, Nature, 534, 91-94, 10.1038/nature17646,
943   2016.
944

Atmospheric
Chemistry
and Physics
Discussions

945   Marey, H. S., Hashisho, Z., Fu, L., and Gille, J.: Spatial and temporal variation in CO over Alberta using
946   measurements from satellites, aircraft, and ground stations, Atmos. Chem. Phys., 15, 3893-3908,
947   10.5194/acp-15-3893-2015, 2015.
948
949   Markovic, M. Z., VandenBoer, T. C., and Murphy, J. G.: Characterization and optimization of an online
950   system for the simultaneous measurement of atmospheric water-soluble constituents in the gas and
951   particle phases, Journal of Environmental Monitoring, 14, 1872-1884, 10.1039/c2em00004k, 2012.
952
953   Masliyah, J., Zhou, Z. J., Xu, Z. H., Czarnecki, J., and Hamza, H.: Understanding water-based bitumen
954   extraction from athabasca oil sands, Can. J. Chem. Eng., 82, 628-654, 10.1002/cjce.5450820403, 2004.
955
956   McLinden, C. A., Fioletov, V., Boersma, K. F., Krotkov, N., Sioris, C. E., Veefkind, J. P., and Yang, K.: Air
957   quality over the Canadian oil sands: A first assessment using satellite observations, Geophys. Res. Lett.,
958   39, 8, 10.1029/2011gl050273, 2012.
959
960   Miller, S. M., Matross, D. M., Andrews, A. E., Millet, D. B., Longo, M., Gottlieb, E. W., Hirsch, A. I., Gerbig,
961   C., Lin, J. C., Daube, B. C., Hudman, R. C., Dias, P. L. S., Chow, V. Y., and Wofsy, S. C.: Sources of carbon
962   monoxide and formaldehyde in North America determined from high-resolution atmospheric data,
963   Atmos. Chem. Phys., 8, 7673-7696, 10.5194/acp-8-7673-2008, 2008.
964
965   Min, K. E., Pusede, S. E., Browne, E. C., LaFranchi, B. W., and Cohen, R. C.: Eddy covariance fluxes and
966   vertical concentration gradient measurements of NO and NO2 over a ponderosa pine ecosystem:
967   observational evidence for within-canopy chemical removal of NOx, Atmos. Chem. Phys., 14, 5495-5512,
968   10.5194/acp-14-5495-2014, 2014.
969
970   Nara, H., Tanimoto, H., Tohjima, Y., Mukai, H., Nojiri, Y., Katsumata, K., and Rella, C. W.: Effect of air
971   composition (N-2, O-2, Ar, and H2O) on CO2 and CH4 measurement by wavelength-scanned cavity ring-
972   down spectroscopy: calibration and measurement strategy, Atmos. Meas. Tech., 5, 2689-2701,
973   10.5194/amt-5-2689-2012, 2012.
974
975   Nimana, B., Canter, C., and Kumar, A.: Energy consumption and greenhouse gas emissions in the
976   recovery and extraction of crude bitumen from Canada's oil sands, Appl. Energy, 143, 189-199,
977   10.1016/j.apenergy.2015.01.024, 2015a.
978
979   Nimana, B., Canter, C., and Kumar, A.: Energy consumption and greenhouse gas emissions in upgrading
980   and refining of Canada's oil sands products, Energy, 83, 65-79, 10.1016/j.energy.2015.01.085, 2015b.
981
982   Detailed facility information: http://www.ec.gc.ca/inrp-npri/donnees-
983   data/index.cfm?do=facility_information&lang=En&opt_npri_id=0000002274&opt_report_year=2013,
984   access: April 13, 2017, 2013.
985
986   Odame-Ankrah, C. A.: Improved detection instrument for nitrogen oxide species, Ph.D., Chemistry,
987   University of Calgary, http://hdl.handle.net/11023/2006, Calgary, 2015.
988
989   Onasch, T. B., Trimborn, A., Fortner, E. C., Jayne, J. T., Kok, G. L., Williams, L. R., Davidovits, P., and
990   Worsnop, D. R.: Soot Particle Aerosol Mass Spectrometer: Development, Validation, and Initial
991   Application, Aerosol Sci. Technol., 46, 804-817, 10.1080/02786826.2012.663948, 2012.
992

Atmospheric
Chemistry
and Physics
Discussions

993
994
995   Parajulee, A., and Wania, F.: Evaluating officially reported polycyclic aromatic hydrocarbon emissions in
996   the Athabasca oil sands region with a multimedia fate model, Proceedings of the National Academy of
997   Sciences, 111, 3344-3349, 10.1073/pnas.1319780111, 2014.
998
999   Paul, D., and Osthoff, H. D.: Absolute Measurements of Total Peroxy Nitrate Mixing Ratios by Thermal
1000   Dissociation Blue Diode Laser Cavity Ring-Down Spectroscopy, Anal. Chem., 82, 6695-6703,
1001   10.1021/ac101441z, 2010.
1002
1003   Penner, T. J., and Foght, J. M.: Mature fine tailings from oil sands processing harbour diverse
1004   methanogenic communities, Canadian Journal of Microbiology, 56, 459-470, 10.1139/w10-029, 2010.
1005
1006   Percy, K. E.: Ambient Air Quality and Linkage to Ecosystems in the Athabasca Oil Sands, Alberta, Geosci.
1007   Can., 40, 182-201, 10.12789/geocanj.2013.40.014, 2013.
1008
1009   Peters, T. M., and Leith, D.: Concentration measurement and counting efficiency of the aerodynamic
1010   particle sizer 3321, J. Aerosol Sci., 34, 627-634, 10.1016/s0021-8502(03)00030-2, 2003.
1011
1012   Quagraine, E. K., Headley, J. V., and Peterson, H. G.: Is biodegradation of bitumen a source of recalcitrant
1013   naphthenic acid mixtures in oil sands tailing pond waters?, J. Environ. Sci. Health Part A-Toxic/Hazard.
1014   Subst. Environ. Eng., 40, 671-684, 10.1081/ese-200046637, 2005.
1015
1016   Rooney, R. C., Bayley, S. E., and Schindler, D. W.: Oil sands mining and reclamation cause massive loss of
1017   peatland and stored carbon, Proc. Natl. Acad. Sci. U.S.A., 109, 4933-4937, 10.1073/pnas.1117693108,
1018   2012.
1019
1020   RStudio Boston, M.: Integrated development environment for R, 2017.
1021
1022
1023
1024   Shahimin, M. F. M., and Siddique, T.: Sequential biodegradation of complex naphtha hydrocarbons
1025   under methanogenic conditions in two different oil sands tailings, Environ. Pollut., 221, 398-406,
1026   10.1016/j.envpol.2016.12.002, 2017.
1027
1028   Siddique, T., Fedorak, P. M., and Foght, J. M.: Biodegradation of short-chain n-alkanes in oil sands
1029   tailings under methanogenic conditions, Environ. Sci. Technol., 40, 5459-5464, 10.1021/es060993m,
1030   2006.
1031
1032   Siddique, T., Gupta, R., Fedorak, P. M., MacKinnon, M. D., and Foght, J. M.: A first approximation kinetic
1033   model to predict methane generation from an oil sands tailings settling basin, Chemosphere, 72, 1573-
1034   1580, 10.1016/j.chemosphere.2008.04.036, 2008.
1035
1036   Siddique, T., Penner, T., Semple, K., and Foght, J. M.: Anaerobic Biodegradation of Longer-Chain n-
1037   Alkanes Coupled to Methane Production in Oil Sands Tailings, Environm. Sci. Technol., 45, 5892-5899,
1038   10.1021/es200649t, 2011.
1039

Atmospheric
Chemistry
and Physics
Discussions

1040   Siddique, T., Penner, T., Klassen, J., Nesbo, C., and Foght, J. M.: Microbial Communities Involved in
1041   Methane Production from Hydrocarbons in Oil Sands Tailings, Environ. Sci. Technol., 46, 9802-9810,
1042   10.1021/e53022024, 2012.
1043
1044   Simpson, I. J., Blake, N. J., Barletta, B., Diskin, G. S., Fuelberg, H. E., Gorham, K., Huey, L. G., Meinardi, S.,
1045   Rowland, F. S., Vay, S. A., Weinheimer, A. J., Yang, M., and Blake, D. R.: Characterization of trace gases
1046   measured over Alberta oil sands mining operations: 76 speciated C2–C10 volatile organic compounds
1047   (VOCs), CO_2, CH_4, CO, NO, NO_2, NO_y, O_3 and SO_2, Atmos. Chem. Phys., 10, 11931-11954, 10.5194/acp-10-
1048   11931-2010, 2010.
1049
1050   Small, C. C., Cho, S., Hashisho, Z., and Ulrich, A. C.: Emissions from oil sands tailings ponds: Review of
1051   tailings pond parameters and emission estimates, J. Pet. Sci. Eng., 127, 490-501,
1052   10.1016/j.petrol.2014.11.020, 2015.
1053
1054
1055
1056   Thurston, G. D., and Spengler, J. D.: A quantitative assessment of source contributions to inhalable
1057   particulate matter pollution in metropolitan Boston, Atmos. Environ., 19, 9-25, 10.1016/0004-
1058   6981(85)90132-5, 1985.
1059
1060   Thurston, G. D., Ito, K., and Lall, R.: A source apportionment of U.S. fine particulate matter air pollution,
1061   Atmos. Environ., 45, 3924-3936, 10.1016/j.atmosenv.2011.04.070, 2011.
1062
1063   Tokarek, T. W., Huo, J. A., Odame-Ankrah, C. A., Hammoud, D., Taha, Y. M., and Osthoff, H. D.: A gas
1064   chromatograph for quantification of peroxycarboxylic nitric anhydrides calibrated by thermal
1065   dissociation cavity ring-down spectroscopy, Atmos. Meas. Tech., 7, 3263-3283, 10.5194/amt-7-3263-
1066   2014, 2014.
1067
1068   Tokarek, T. W., Brownsey, D. K., Jordan, N., Garner, N. M., Ye, C. Z., Assad, F. V., Peace, A., Schiller, C. L.,
1069   Mason, R. H., Vingarzan, R., and Osthoff, H. D.: Biogenic Emissions and Nocturnal Ozone Depletion
1070   Events at the Amphitrite Point Observatory on Vancouver Island, Atmosphere-Ocean, 1-12,
1071   10.1080/07055900.2017.1306687, 2017.
1072
1073   Wang, S. C., and Flagan, R. C.: Scanning electrical mobility spectrometer, Aerosol Sci. Technol., 13, 230-
1074   240, 10.1080/02786829008959441, 1990.
1075
1076   Wang, X. L., Chow, J. C., Kohl, S. D., Percy, K. E., Legge, A. H., and Watson, J. G.: Characterization of
1077   PM2.5 and PM10 fugitive dust source profiles in the Athabasca Oil Sands Region, J. Air Waste Manag.
1078   Assoc., 65, 1421-1433, 10.1080/10962247.2015.1100693, 2015.
1079
1080   Wang, X. L., Chow, J. C., Kohl, S. D., Percy, K. E., Legge, A. H., and Watson, J. G.: Real-world emission
1081   factors for Caterpillar 797B heavy haulers during mining operations, Particuology, 28, 22-30,
1082   10.1016/j.partic.2015.07.001, 2016.
1083
1084   Warren, L. A., Kendra, K. E., Brady, A. L., and Slater, G. F.: Sulfur Biogeochemistry of an Oil Sands
1085   Composite Tailings Deposit, Front. Microbiol., 6, 14, 10.3389/fmicb.2015.01533, 2016.
1086

Watson, J. G., Chow, J. C., Wang, X., Zielinska, B., Kohl, S. D., and Gronstal, S.: Characterization of real-world emissions from nonroad mining trucks in the athabasca oil sands region during september, 2013.

WBEA: WBEA annual report 2013, Wood Buffalo Environmental Association, 2013.

Whaley, C., Makar, P. A., Shephard, M. W., Zhang, L., Zhang, J., Zheng, Q., Akingunola, A., Wentworth, G. R., Murphy, J. G., Kharol, S. K., and Cady-Pereira, K. E.: Contributions of natural and anthropogenic sources to ambient ammonia in the Athabasca Oil Sands and north-western Canada, Atmos. Chem. Phys., submitted, 2017.

Wilson, N. K., Barbour, R. K., Chuang, J. C., and Mukund, R.: Evaluation of a real-time monitor for fine particle-bound PAH in air, Polycycl. Aromat. Compd., 5, 167-174, 10.1080/10406639408015168, 1994.

Yeh, S., Jordaan, S. M., Brandt, A. R., Turetsky, M. R., Spatari, S., and Keith, D. W.: Land Use Greenhouse Gas Emissions from Conventional Oil Production and Oil Sands, Environ. Sci. Technol., 44, 8766-8772, 10.1021/es1013278, 2010.

Zhang, Y., Wang, Y., Chen, G., Smeltzer, C., Crawford, J., Olson, J., Szykman, J., Weinheimer, A. J., Knapp, D. J., Montzka, D. D., Wisthaler, A., Mikoviny, T., Fried, A., and Diskin, G.: Large vertical gradient of reactive nitrogen oxides in the boundary layer: Modeling analysis of DISCOVER-AQ 2011 observations, Journal of Geophysical Research: Atmospheres, 1922–1934, 10.1002/2015jd024203, 2016.